Electrochimica Acta 374 (2021) 137929

Contents lists available at ScienceDirect

Electrochimica Acta

journal homepage: www.elsevier.com/locate/electacta

Electrochemical detection of trace silver

Kequan Xu[#], Clara Pérez-Ràfols[#], Maria Cuartero, Gaston A. Crespo[*]

Department of Chemistry, School of Engineering Science in Chemistry, Biotechnology and Health, KTH Royal Institute of Technology, Teknikringen 30, Stockholm SE-100 44, Sweden

ARTICLE INFO

Article history:
Received 8 December 2020
Revised 5 February 2021
Accepted 6 February 2021
Available online 10 February 2021

Keywords:
Silver
Trace amounts
Ion-selective electrodes
Stripping voltammetry

ABSTRACT

Increasing utilization of silver and silver nanoparticles (AgNPs) in daily processes and products has led to a significant growth in scientific interest in methods for monitoring silver. In particular, the amount of silver ions (Ag^+) released to the environment is known to have a detrimental effect on aquatic ecology, and thus some control actions have been implemented in recent years; for example, the manufacturing industry is now required to control and certify the quantity of AgNPs present in products. Electrochemical sensors are well suited to the task of silver monitoring due to several beneficial properties, including low costs, fast measurements, and facile adaptation to miniaturized, portable instrumentation. The predominant method for electrochemical silver determination involves potentiometric ion selective electrodes (ISEs) and voltammetric measurements. Reviewing the literature of the last ten years reveals significant improvements in the analytical performance of electrochemical sensors, mainly related to the development of new protocols, selective receptors, and electrode materials. Remarkably, ISEs with limits of detection (LOD) in the nanomolar range have been reported, employing careful control of ion fluxes across the membrane interfaces. What's more, sub-nanomolar LODs are attainable by stripping voltammetry using either ligand-based deposition strategies or thin layer membranes coupled to conducting polymers. Selectivity has also been optimized through the membrane composition of ISEs, with special focus on Ag^+ ionophores. Furthermore, novel voltammetric methods allow for discrimination between Ag^+ and AgNPs. However, there is still a dearth of studies applying such electrochemical sensors to on-site water analysis, and hence, further research is needed in order to translate these laboratory scale achievements to real-world contexts. Overall, this review describes the state-of-the-art in electrochemical silver detection, and provides a comprehensive description of those aspects contributing to the further development and improvement of analytical performance.

1. Introduction

Silver is a naturally occurring metal whose extraordinary properties have been known to mankind since antiquity, which currently finds use in such diverse applications as electronics, explosives, photography, and medicine. In addition, the relatively non-reactive and antibacterial nature of silver in its metallic form, together with its luster, have encouraged its use in the fabrication of utensils, hollowware, and jewelry. As a result of this versatility, the market demand for silver has exceeded 30,000 tons per year since 2010 [1], which has been accompanied by a remarkable release of silver into the environment. The non-natural presence of silver is a cause for concern, given that it is a non-biodegradable metal able to persist in the environment for long time periods. Furthermore, anthropogenic emissions to the environment induce perturbations in silver speciation, which drastically affects its geochemical (mobility, reactivity) and biological (bioavailability, toxicity) behavior [2]. Whereas silver naturally occurs mainly in the form of highly insoluble and immobile oxides and sulfides [3], these changes in speciation may result in the release of these previously trapped silver ions (Ag^+), which is especially troubling given the extreme toxicity of silver (comparable to that of mercury) [4]. In humans, severe exposure to Ag^+, known as argyria, causes skin and hair to turn blue-gray [3-5].

Silver in the form of nanoparticles (AgNPs) is of particular interest, as it constitutes one of the most commonly used engineered nanomaterials and finds use in many applications and products, such as water filters, paints, textile, food packaging, detergents, biosensors, and biomedicines [6,7]. In order for AgNPs to satisfy

* Corresponding author.
E-mail address: gacp@kth.se (G.A. Crespo).
Sharing first authorship.

https://doi.org/10.1016/j.electacta.2021.137929

Table 1
Silver levels reported for different applications.

Description	Specie	Concentration range	Ref
Drinking water recommended maximum levels	Total Ag	0.93 µM	[33]
Environmental studies			
Genesee River, USA - Groundwater	Total Ag	< 92 – 1020 pM	[36]
Phulali Canal, Pakistan – fresh water receiving municipal and industrial effluents	Total Ag	64 – 504 nM	[37]
Ocean water (global locations)	Dissolved Ag	< 0.24 – 307 pM	[32]
Influents in wastewater treatment plants (Germany)	Total Ag	3 – 28 nM	[38]
Sperm whales (global study)	Total Ag	0.93 – 1.14 ng/g	[39]
AgNPs released from paint used in outdoor facades	AgNP	< 0.74 – 1854 nM	[40]
Predicted AgNPs concentration in surface water in 2020	AgNP	0.003 – 16.7 nM	[41]
Product manufacturing			
Toothpaste	Total Ag	0.044 – 61 µg/g	[35]
Detergent	Total Ag	0.055 – 27 µg/g	[35]
Antibacterial spray	Total Ag	0.04 – 94 µg/g	[35]
AgNPs synthesis			
Humic acid induced	Ag^+	0.01 – 1 mM	[14]
Fulvic acid induced	Ag^+	0.005 – 1 mM	[15]
Sunlight induced in the presence of chloride	Ag^+	0.05 – 0.1 mM	[42]
Sunlight induced in the presence of organic matter	Ag^+	10 – 200 mM	[16]
Studies/applications related to AgNPs			
Study of AgNPs toxicity	AgNP	0.006 – 51 µM	[43]
Use of AgNPs to study protein interactions	AgNP	0.9 – 50 nM	[44]
Release of Ag from AgNPs coated surgical sutures	Total Ag	2.6 – 26 µM	[45]
Evaluation of the disinfectant performance	AgNP	9.2 – 185 nM	[46]

the expected requirements for the targeted application, precise control of the amount of silver present is crucial. As with Ag^+, toxic effects have been reported for AgNPs when discharged to the environment [7,8]; it is therefore essential to have access to reliable analytical methods for the detection and quantification of silver.

The current reference method for the determination of silver is inductively coupled plasma (ICP) with either mass spectrometry (ICP-MS) [9-11] or optical emission spectrometry (ICP-OES) [11-13]. The limit of detection (LOD) for silver ions using these methods falls easily within the nanomolar level, and they provide several desirable features for such analyses, including wide linear range of response (LRR), high accuracy and sensitivity, simultaneous multi-element characterization, and the possibility to obtain isotopic information. However, the equipment required for ICP is bulky and expensive, some samples may require pretreatment, and the analysis itself requires a constant supply of inert gas, all of which effectively limits the use of these techniques to centralized laboratory analysis. For many applications (*e.g.* quality control in manufacturing, environmental assessment of wastewaters, real-time monitoring of formation and dissolution of AgNPs) [14-17] real-time and/or on-site measurements are highly desirable. Electrochemical sensors offer a far greater scope for such decentralized analysis, being easily adaptable for miniaturization and portability, and can even be used in the analysis of extremely low-volume samples [18,19]. Particular examples of the successful application of electrochemical sensors to decentralized analysis include the use of fluidic based submersible probes for the long-term determination of pH, calcium and carbonate in seawater [20] and a profiling ion analyzer (PIA) for high depth resolution of pH and ammonium in freshwater [21,22]. For more detailed information regarding decentralized electrochemical analysis the reader is referred to the following reviews [19,23]. In the case of silver detection, several electrochemical sensors have been reported, mostly in the form of ion selective electrodes (ISE) [24-27] or voltammetric sensors [28-31]. Although early proposed electrochemical sensors offered significantly inferior sensitivity and LOD to that provided by ICP-MS, important advances in analytical performance have been achieved over the last decade, positioning electrochemical sensing as a supremely viable technique for on-site silver analysis [32]. An additional benefit can be obtained by the use of electrochemical sensors, in that they allow direct speciation among different silver species; a feature that can only be achieved with ICP when coupled to a suitable separation technique (usually in the form of chromatography) [11].

In order to understand the necessity for decentralized silver monitoring, it is important to consider the levels of silver associated with the most common applications. Some specific examples of silver levels somehow linked to the need for decentralized analysis (*e.g.* environmental control, product manufacturing, AgNPs) are collected in Table 1. In drinking water, silver is categorized within the Secondary Maximum Contaminant Levels (SMCL) by the Environmental Protection Agency (EPA) [33]. As such, only non-mandatory drinking water quality standards have been established for silver, with the maximum level set at 0.93 µM. However, there is no clear evidence that levels below this limit necessarily prevent argyria in humans, especially if we consider that drinking water is not the only source of silver to which humans are daily exposed [33]. In fact, the presence of silver has been reported in several biological fluids, with levels ranging from 0 to 2.4 nM and from 0 to 3.0 nM in blood and urine, respectively [34]. Even higher values are expected for patients using silver-coated prostheses [34]. From an environmental perspective, silver surveillance is important due to its toxicity to aquatic organisms. Typical silver concentration in natural water ranges between 0.28 pM and 4.6 nM [6], which means that an analytical technique with an unusually broad range of response is required for its analysis. A wide concentration range is also expected for AgNPs in samples connected to synthetic procedures (up to mM) and applications (nM), *e.g.* surgical sutures, study of protein interactions. Similar silver levels are also common in product manufacturing (*e.g.* sanitizers, toothpaste) [35].

This work critically reviews the advances in silver electrochemical sensing achieved in the last decade, taking into account the mentioned criteria pertaining to silver concentrations and decentralized analysis. Beyond providing an updated assortment of papers on that topic, this review particularly focuses on those achievements that allow lowering LODs and/or facilitate implementation in on-site analysis. Altogether, we consider that the analysis of the selected works will stimulate future progress in decentralized silver monitoring; if we have obviated any manuscripts reporting on electrochemical silver sensors, it was not our intention to undervalue those works. All data presented herein were acquired from the original sources (published papers), and it was not

our goal when analyzing the analytical parameters to criticize the manner in which they were calculated.

2. Potentiometric determination of silver

Generally, the concept of potentiometric determination of silver can be considered synonymous with ion-selective electrodes (ISEs), tailored for Ag^+ detection. To the best of our knowledge, the first Ag^+ selective electrode was reported in 1968 and was based on Ag/Ag_2S crystal membranes [47]. This electrode presented a Nernstian response from 0.1 mM to 0.1 M Ag^+ concentration, and unlike many other sulfide-based ISEs it showed a very high primary ion selectivity, only weakly responding to other transition metal ions with the exception of Hg^{2+} [48]. In all probability this selectivity played an important role in delaying the development of liquid membrane ISEs for $Ag^+$with respect to other analytes. It was not until 1986 that Lai and Shih demonstrated the first ISE based on a selective membrane for silver [49]. The electrode was of inner-filling-solution type and contained a dithia-crown ether as Ag^+ ionophore. The electrode displayed a sub-Nernstian response (slope of 40 mV), LRR from 10^{-5} to 10^{-1} M, and LOD of 1 μM. In terms of selectivity, the highest interferences were observed for Hg^{2+}, Fe^{3+}, Mg^{2+} and Na^+ ($\log K^{pot}_{Ag^+,M^{n+}}$ = −0.11, −0.06, −1.55 and −1.3, respectively). Following this breakthrough, efforts were directed towards ameliorating both the LOD and the selectivity, in the main following two strategies: (i) optimization of the membrane composition with special emphasis on the search for new Ag^+ ionophores to improve the selectivity; and (ii) the control of ion fluxes across the membrane interfaces, primarily to optimize the LOD and bring it to the levels required for real-sample Ag^+ detection.

Table 2 collects potentiometric ISEs for Ag^+ detection reported since 2010. These electrodes are all based on a silver-selective membrane, employing different ionophores (or selective receptors). It is important to mention that the appearance of silver-selective electrodes in the solid-contact format dates from 2001 [50], almost 10 years after the first demonstrations of conducting polymers as effective ion-to-electron transducers in ISEs [51]. Whatever the configuration of the electrode, the use of a plasticized polymeric silver selective membrane is a constant feature in the collected potentiometric ISEs. The reported membranes usually contain the ionophore (ranging from 10 to 80 mmol kg^{-1} membrane), a cation exchanger (5–40 mmol kg^{-1}), a polymer (25–35 wt%) and a plasticizer (55–67 wt%); some of the reported membranes do not contain a cation exchanger. A range of common cation exchangers have been applied in potentiometric ISEs: sodium tetraphenylborate (NaTPB) [52], potassium tetrakis p-(chlorophenyl)borate (KTpClPB) [53,54] and sodium tetrakis-[3,5-bis(trifluoromethyl)phenyl]borate (NaTFPB) [55,56]. For the polymeric matrix polyvinyl chloride (PVC) is the preferred polymer, and typical plasticizers include 2-nitrophenyl octyl ether (o-NPOE) [54,56,57], dioctyl phthalate (DOP) [53,58], dibutyl sebacate (DBS) [59], dibutyl phthalate (DBP) [52,60] and dioctyl adipate (DOA) [61]. Overall, we could not realize any general benefit of using a specific cation exchanger or plasticizer in silver-selective electrodes, although fluorous polymers seem to favor Ag^+ coordination in conjunction with certain types of ionophores (see below) [62].

Regarding the ionophore, there are two principal aspects to be considered: its chemical and physical nature, and the molar ratio ionophore: cation exchanger in the membrane. Receptors that have been demonstrated as silver ionophores include calixerene derivatives [53,63,64], Schiff bases [60,65,66], azathioether derivatives [56,67], podands [68,69], porphyrin derivatives [25,70], cholane derivatives [71], other macrocyclic compounds [72,73] and, more recently, similar compounds coupled to nanomaterials [74,75]. Representative examples of each group are displayed in Fig. 1. Seemingly, the receptors most frequently utilized are calix[4]arene based compounds; indeed, one commercially available ionophore showing an excellent selectivity profile ($\log K^{pot}_{Ag^+,M^{n+}}$ = −2.5 for Hg^{2+}; −4.7 for K^+ and Pb^{2+}; −5 for Na^+ and Ni^{2+}; < −5 for NH_4^+, Cu^{2+}, $Cd^{2+}$and Zn^{2+} in a membrane containing KTpClPB and BBPA as plasticizer and calculated using the fixed interference method (FIM)) is labeled as O,O″-bis[2-(methylthio)ethyl]–tert-butylcalix[4]arene (also known as silver ionophore IV) [63].

An important number of new publications appearing in the literature related to ISEs for $Ag^+$are, still, concerned with the development of new ionophores. In this context, several structural features are thought to be critical to achieve selective binding of the ionophore for Ag^+, with the incorporation of soft donor atoms (*e.g.* S, N) and π-coordinating centers, and geometrical arrangement among the most important aspects [64]. The presence of carbonyl groups generally favors coordination to alkali metals, whereas the incorporation of substituents containing π-electrons or sulfur and nitrogen atoms increases the interaction with soft transition metals (*i.e.*, Hg^{2+}, Ag^+, Cu^{2+}). Szigeti et al. demonstrated that higher Ag^+ selectivity is achieved with calix[4]arene ionophores incorporating sulfur donor atoms than π-coordinating centers [76]. Thus, of ten different calix[4]arene derivatives tested, those based on π-coordinating centers showed logarithmic selectivity coefficients (calculated using the separate solution method, SSM) lower than −6 for Na^+, H^+ and Ca^{2+}, while those incorporating sulfur atoms presented $\log K^{pot}_{Ag^+,M^{n+}}$ between −6.5 and −13 for the same interfering cations [76]. In a later study, substituents containing donor atoms were further investigated by Janrungroatsakul et al., (Fig. 2), demonstrating that the presence of two substituents on opposing phenolic groups of calix[4]arene (compounds II, III) results in lower susceptibility to interferences than displayed by monosubstituted calix[4]arenes (compounds I, IV) [77]. Importantly, the highest selectivity was achieved with two benzothiazole substituents (compound III, Fig. 2), which provided a $\log K^{pot}_{Ag^+,M^{n+}}$ < −3 for all tested interfering cations, except for Hg^{2+} which gave $\log K^{pot}_{Ag^+,M^{n+}}$ ~ −2.

Crown ethers *per se* generally present high affinity to alkali and alkaline earth metal ions, whereas substitution of oxygen atoms by nitrogen and/or sulfur provides higher affinity towards transition and heavy metal ions [78,79]. Zhang et al. explored the use of nine monoazathiacrown ethers as Ag^+ ionophores (Fig. 3), studying the effect of total ring number (20, 21, 22 for compounds V, VI, VII; 17, 18, 19 for compounds VIII, IX, X; 19, 20, 21 for compounds XI, XII, XIII) and number of sulfur atoms (5 for compounds V, VI, VII, 4 for others) present in the ring [80]. The authors observed that selectivity towards Ag^+ depended on the number of sulfur atoms present in the ring system (more sulfur provides enhanced selectivity), and the flexibility of the ring. More flexible rings allowed for the ionophore to more easily contort in order to form stable complexes with ions such as Hg^{2+}, resulting in poorer selectivity. In this case, the best selectivity ($\log K^{pot}_{Ag^+,M^{n+}}$ = −2.5 (Hg^{2+}), −8.2 (K^+), −8.4 (Pb^{2+}) and lower than −9 for all other tested ions using the SSM) was achieved with a 2,2′-thiodiethanethiol derivative containing five sulfur atoms and a total ring number of 22 atoms (compound VII, Fig. 3). An optimized membrane containing PVC (33 wt%), o-NPOE (66 wt%), ionophore (0.7 wt%) and NaTFPB (0.3 wt%, corresponding to a 4:1 ionophore: NaTFPB molar ratio) resulted in a very respectable LOD of 0.22 nM and a near-Nernstian response (slope of 54.5 mV dec^{-1}) up to 10^{-5} M Ag^+ concentration.

Although most of the reported Ag^+ ionophores are based on macrocyclic compounds, a few non-macrocycle ionophores have also been reported. The group of Nam evaluated the suitability of tweezer-type ionophores based on cholic, deoxycholic and chenodeoxycholic acid derivatives as well as 7-deoxycholic amide and cholane derivatives [71,81]. Compared to analogous compounds containing a single binding site, tweezer-type ionophores

Table 2
Potentiometric silver-selective electrodes.

Type of electrode	Ionophore	Membrane composition	Analytical performance	Ag^+/Na^+ selectivity $\log K^{pot}_{Ag^+,Na^+}$	Application	Ref
IFS	5-(4-dimethylaminobenzylidene) rhodanine	5 wt.% I, 60 wt.% DOP, 35 wt.% PVC	LOD: 1 μM, LRR: 1 μM – 0.1 mM, t_r: 20 s	NS	None	[58]
IFS	thioether–amide–amine based ionophores	4 wt.% I, 63 wt.% o-NPOE, 33 wt.% PVC	LOD: 60 μM, LRR: 100 μM – 100 mM, t_r: < 15 s	−1.4	Titration of Ag^+	[57]
IFS	p-tert-butylthiacalix[4]arene derivative	1.8 wt.% I, 63.6 wt.% DBS, 34.5 wt.% PVC, 1.0 wt.% NaTFPB	LOD: 5 nM, LRR: 7 μM – 8 mM, t_r: 10 – 20 s	−2.0	Titration of Ag^+	[59]
IFS	p-tert-butylcalix[4]arene	1.00 wt.% I, 65.97 wt.% DOP, 32.99 wt.% PVC, 0.04 wt.% KTpClPB	LOD: 0.1 μM, LRR: 0.5 μM – 1 mM	−4.01	Titration of Cl^- in water samples, determination of vitamin C	[53]
IFS	calix[4]arene derivatives	1.0 wt.% I, 66.0 wt.% o-NPOE, 33.0 wt.% PVC, 75 mol% KTClPB relative to I	LOD: 0.48 μM, LRR: 1 μM – 10 mM	−6.7	Detect DNA hybridization	[77]
IFS	24,26-dihydroxy-25,27-bis(1-ethoxycarbonylmethoxy1,2,3-triazole-4–methoxy)-p-tert-butylcalix[4]arene	2.0 wt.% I, 66. wt.% o-NPOE, 33.0 wt.% PVC, 50 mol% KTClPB relative to I	NS	−6.7	NS	[121]
IFS	aza-thioether crown containing a 1,10-phenanthroline subunit silver(I) ion-imprinted polymer (IIP)	9.2 wt.% I, 61.3 wt.% o-NPOE, 27.6 wt.% PVC, 1.9 wt.% NaTFPB	LOD: 1.2 nM, LRR: 5 μM – 100 mM, t_r: 25 – 60 s	NS	Spiked Ag^+ water samples	[56]
IFS	diamide 7,10,13-triaza-1-thia-4,16-dioxa-20,24-dimethyl-2,3; 17,18-dibenzo-cyclooctadecane-6,14-dione	6.0 wt.% I, 56.0 wt.% o-NPOE, 30.0 wt.% PVC, 8.0 wt.% OA	LOD: 1 μM, LRR: 2 μM – 10 mM, t_r: < 55 s	NS	Detection of Ag^+ in photographic and radiographic films	[72]
IFS	1,13-bis(8-quinolyl)−1,4,7,10,13-pentaoxatridecane	5.3 wt.% I, 4.5 wt.% NaTPB, 30.0 wt.% PVC, 60.2 wt.% DBP	LOD: 0.9 μM, LRR: 1 μM – 100 mM, t_r: 15 s	−3.24	Spiked Ag^+ distilled water samples	[52]
IFS	2,2′-(1E,1′E)-(1,1′-binaphthyl-2,2′-diylbis(azan-1-yl-1-ylidene))bis(methan-1-yl-1-ylidene)diphenol	1.0 wt.% I, 60.2 wt.% o-NPOE, 33.0 wt.% PVC, 50.0 mol.% KTClPB	LOD: 0.34 μM, LRR: 1 μM – 10 mM, t_r: 3 s	−3.6	Spiked Ag^+ tap water samples	[122]
IFS	(N2E,N2′E)-N2,N2′-Bis(Thiophen-2-ylmethylene)−1,1′-Binaphthyl-2,2′-Diamine	1.0 wt.% I, 66.0 wt.% DOA, 33.0 wt.% PVC	LOD: 40 nM, LRR: 0.1 μM – 10 mM, t_r: 9 s	−3.6	NS	[61]
IFS	9,10,20,25-tetrahydro-5H,12H-tribenzo[*b,n,r*][1,7,10,16,4,13]tetrathiadiaza cycloicosine 6,13-(7H,14H)–dione	1.0 wt.% I, 65.7 wt.% o-NPOE, 32.9 wt.% PVC, 0.4 wt.% NaTFPB	LOD: 55 nM, LRR: 1 μM – 1 mM, t_r: < 15 s	−8.64	Titration of chloride in water	[55]
IFS	9,10,12,13,24,25-Hexahydro-5H,15H,23Hdibenzo[*b,q*][1,7,10,13,19,4,16]-pentathiadiazacyclodocosine 6,16(7H,17H)-dione	0.7 wt.% I, 66.1 wt.% o-NPOE, 33.0 wt.% PVC, 0.3 wt.% NaTFPB	LOD: 0.22 nM, LRR: 1 nM - 10 μM	−9.4	Spiked Ag^+ tap water samples	[80]
IFS	N,N'-Bis(pyridin-2-ylmethylene)benzene-1,2-diamine	1.0 wt.% I, 66.0 wt.% o-NPOE, 33.0 wt.% PVC, 50 mol% KTpClPB relative to I	LOD: 0.23 μM, LRR: 0.1 μM – 1 mM, t_r: 10 s	NS	NS	[123]
IFS	1,3-Bis(2-ethoxyphenyl)Triazene	1.5 wt.% I, 65.0 wt.% TEHP, 33.0 wt.% PVC, 0.5 wt.% NaTFPB	LOD: 85 nM, LRR: 0.32 μM – 100 mM, t_r: 12 s	−3.37	Spiked Ag^+ tap, well, river, waste, mineral water samples	[124]
IFS	N,N'-Bis(3-methyl-1-phenyl-4-benzylidine-5-pyrazolone)propylenediamine	2.2 wt.% I, 64.7 wt.% DBP, 32.3 wt.% PVC, 0.8 wt.% KTpClPB	LOD: 0.2 μM, LRR: 1 μM – 100 mM, t_r: 5 – 30 s	−4.7	Detection of Ag^+ in radiographic films	[60]
IFS	Fullerene-Based 2-aminopyridine 3–hydroxy benzaldehyde	5.0 wt.% I, 63.0 wt.% DOP, 30.0 wt.% PVC, 2.0 wt.% NaTFPB	LOD: 0.1 μM, LRR: 0.5 μM – 100 mM, t_r: < 10 s	$6.1 \bullet 10^{-6}$ (MPM)	Biosensing of glucose	[74]
IFS	ionophore–gold nanoparticle conjugate	NS	LOD: 10 nM, LRR: 1 mM – 10 nM	−5.3	NS	[75]
SS-CPE	(Z)−2-(2-((3-(2-hydroxyphenyl)−5-(p-tolyl)−1H-pyrrol-2-yl)imino)−5-(p-tolyl)−2H-pyrrol-3-yl)phenol	2.5 wt.% I, 61.7 wt.% DOS, 34.8 wt.% PVC, 1.0 wt.% KTClPB	LOD: 0.73 μM, LRR: 10 μM – 100 mM, t_r: 3 s	−3.72	Spiked Ag^+ urban, river, spring and some commercially available bottled water samples	[110]

(*continued on next page*)

Table 2 (*continued*)

Type of electrode	Ionophore	Membrane composition	Analytical performance	Ag^+/Na^+ selectivity $\log K^{pot}_{Ag^+,Na^+}$	Application	Ref
SS-CPE	Acetophenone oxime-functionalized glycidyl methacrylate-methyl acrylate copolymer	10 wt.% I, 40 wt.% GP, 35 wt.% PO, 10 wt.% MWCNT	LOD: 0.12 μM, LRR: 0.31 μM – 100 mM, t_r: 5 s	−4.92	Spiked Ag^+ river, lake, tap water samples	[111]
SS-CPE	N,N′-di-(cyclopentadienecarbaldehyde)-1,2-di (o-aminophenylthio) ethane	3.0 wt.% I, 16.0 wt.% GP, 31.0 wt.% RTIL, 50.0 wt.% SGAN	LOD: 0.8 nM, LRR: 2 nM – 20 mM, t_r: 5 s	−4.22	Spiked Ag^+ in urine, blood serum, burning ointment and radiology films	[112]
SS-CPE	N,N'-bis(benzophenone imine)formamidine	6.0 wt.% I, 64.0 wt.% GP, 30.0 wt.% PO	LOD: 50 nM, LRR: 0.2 μM – 20 mM, t_r: < 10 s	−3.27	Titrated mineral water and medicinal sample	[27]
SS-CPE	Single-walled carbon nanotube N-6aminohexylamide	6.07 wt.% I, 30.36 wt.% GP, 63.57 wt.% PO	LRR: 1 μM – 10 mM, t_r: 18 s	NS	NS	[125]
SS-CPE	N-(6-aminohexyl) carboxamide	6.6 wt.% I, 45.0 wt.% GP, 48.4 wt.% PO	LOD: 0.8 μM, LRR: 1 μM – 10 mM, t_r: < 18 s	−2.29	NS	[126]
SS-CPE	2-Acetylbenzimidazole benzoylhydrazone	1.0 wt.% I, 42.4 wt.% GP, 56.6 wt.% DOS	LOD: 70 nM, LRR: 0.11 μM – 1 mM, t_r: 3 s	−2.41	Detection of Ag^+ in radiographic films	[118]
SS-CPE	Thionine	7.0 wt.% I, 53.0 wt.% GP, 30.0 wt.% DPA, 10.0 wt.% GNS	LOD: 4.17 nM, LRR: 8 nM – 10 mM, t_r: 6 s	−5.64	Detection of Ag^+ in acidified river water	[26]
SS-CPE	N1-(1-(pyridin-2-yl)ethylidene)ethane-1,2-diamine-MWCNTMWCNT	9.5 wt.% I, 71.4 wt.% GP, 19.1 wt.% PO	LOD: 0.9 μM, LRR: 1 μM – 100 mM, t_r: 15 s	−4.14	Spiked Ag^+ in reflux tea water	[127]
SS-CPE	MAETEPU-MWCNTs@SiO2	7.6 wt.% I, 71.3 wt.% GP, 21.1 wt.% PO	LOD: 80 n M, LRR: 86 nM – 100 mM, t_r: 20 s	−6.09	Determination of Cl^- ions in water samples	[114]
SS-CPE	B15C5-MWCNTs	8.4 wt.% I, 71.3 wt.% GP, 28.4 wt.% PO	LOD: 0.17 μM, LRR: 0.27 μM – 100 mM, t_r: 15 s	−4.32	Detection of Ag^+ in radiographic films	[115]
SS-CPE	diazo-thiophenol-functionalized silica gel	6.0 wt.% I, 63.5 wt.% GP, 30.5 wt.% PO	LOD: 1 μM, LRR: 1 μM – 100 mM, t_r: 50 s	−5.55	Detection of Ag^+ in radiology films	[128]
SS-CPE	NGO–AuNP–TPC	6.3 wt.% I, 65.1 wt.% GP, 28.6 wt.% PO	LOD: 0.63 μM, LRR: 0.84 μM – 100 mM, t_r: 10 s (1 μM – 100 mM)	−5.19	NS	[115]
SS-CPE	[N,N'(bis[(1-oxoethyl) morpholine-2-carbodithioate])−2,6diaminopyridine]	6.0 wt.% I, 64.0 wt.% GP, 30.0 wt.% PO	LOD: 63 nM, LRR: 80 nM – 15 mM, t_r: 5 s	−3.96(MPM)	Direct determination of tap water and spiked laboratory water	[68]
SS-CPE	1,3,6,10,13-pentaaza-2,14-(2,6-pyridyl)-cyclotetradecane-4,12–dione	8.0 wt.% I, 62.0 wt.% GP, 30.0 wt.% PO, 100 μL SGAN	LOD: 2.5 nM, LRR: 4 nM – 22 mM, t_r: 5 – 15 s	−5.00	Spiked Ag^+ in silver-sulfadiazine cream and radiological film	[68]
SS-CPE	1,3,6,9,11,12-pentaaza-2,13-(2,6-pyridyle)-bicycle[2,2,9]pentadecane-4,11-dione	8.0 wt.% I, 62.0 wt.% GP, 30.0 wt.% PO, 100 uL SGAN	LOD: 0.2 μM, LRR: 0.22 μM – 20 mM, t_r: 5 – 15 s	−5.00	NS	[68]
SS-CPE	1,3-bis(perfluorodecylethylthiomethyl) benzene	3.0 nM I, 1.0 nM NaTFPB	LOD: 38 p M, LRR: 0.1 nM – 1 nM, t_r: 5 s	−12.9	NS	[62]
SS-CPE	PVC-co-VAc	44.3 wt.% I, 55.2 wt.% DBP, 0.5 wt.% NaTFPB	LOD: 4.25 μM, LRR: 10 μM – 100 mM, t_r: 5 – 30 s	NS	Spiked Ag^+ in tap and lake water	[129]
SS-CPE	TEPQA-MCM-41	2 wt.% I, 75 wt.% GP, 23 wt.% PO	LOD: 1 μM, LRR: 1.2 μM – 100 mM,t_r: 5 s	−3.9	Detection of Ag^+ in soil samples, sea water, urine samples	[130]
SS-CPE	graphitic carbon nitride	5.0 wt.% I, 14.3 wt.% n-eicosane, 80.7 wt.% GP	LOD: 0.9 μM, LRR: 1 μM – 100 mM, t_r: 30 s	−3.12	Spiked Ag^+ in river, mineral and sea water	[131]
SS-CW	1,2,4,5-tetrakis-(8-hydroxyquinolinoxymethyl)benzene	4.0 wt.% I, 63.0 wt.% o-NPOE, 33.0 wt.% PVC	LOD: 1 μM, LRR: 10 μM – 100 mM, t_r: 15 s	−1.10	Determination of Ag^+ in various synthetic samples	[103]
SS-CW	Tetraethylthiuram disulfide	6.0 wt.% I, 60.5 wt.% o-NPOE, 33.0 wt.% PVC, 0.5 wt.% NaTFPB	LOD: 1 μM, LRR: 5 μM – 100 mM, t_r: 20 s	−0.6 (MPM)	Titration of F^-,Cl^-,$Br^-$and I^- ions	[104]

(*continued on next page*)

Table 2 (*continued*)

Type of electrode	Ionophore	Membrane composition	Analytical performance	Ag^+/Na^+ selectivity $\log K^{pot}_{Ag^+,Na^+}$	Application	Ref
SS-CP	Zn based porphyrine dimesr into PEDOT dopped with either PSS^- or Cl^-	33.0 wt.% PVC, 66.0 wt.% o-NPOE, 1.0 wt.% porphyrin, 0.2 wt.% KTClPB	LOD: 20 μM, LRR: 100 μM – 70 mM	−4.92	NS	[25]
SS-CP	PANI/SSA	0.5 M aniline, 0.2 M SSA	LOD: 1 nM, LRR: 10 nM – 1 mM	−2.74	Spiked Ag^+ in photographic waste, waste solution	[108]
SS-CP	ARS into polypyrrole	0.1 M pyrrole, 10^{-6} M ARS	LOD: 25 nM, LRR: 50 nM – 6.3 mM, t_r: 10 – 35 s	−3.12	NS	[109]
SS-CP	(O,O''-bis[2-(methylthio)ethyl]-tertbutylcalix[4]arene) into POT	1.7 wt.% GNP@Dit, 65.1 wt.% o-NPOE, 31.8 wt.% PVC, 1.4 wt.% NaTFPB	LOD: 1.26 μM, LRR: 10 μM – 100 mM	−3.9	NS	[107]
SS-CP	o-xylylene-bis(N, N-diisobutyldithiocarbamate) into POT	0.77 wt.% I, 10 wt.% POT, 32.93 wt.% PVC, 65.86 wt.% o-NPOE, 0.44 wt.% NaTFPB	LOD: 19 nM, LRR: 30 nM - 30 μM, t_r: < 20 s	NS	Titration of Cl^- and spiked Ag^+ in tap water and lake water	[106]
SS	o-xylylenebis(N, N-diisobutyldithiocarbamate)	6.00 wt.% I, 65.86 wt.% DOS, 32.93 wt.% PVC, 0.44 wt.% KTFPB	LOD: 0.16 μM, LRR: 1 μM – 1 mM	NS	Kinetic assessment of AgNPs dissolution	[117]

ARS: Alizarin Red S; DBP: dibutyl phthalate; DBS: dibutyl sebacate; DOA: dioctyl adipate; DOP: dioctyl phthalate; DOS: Dioctyl sebacate; DPA: diphenylacetylene; GNS: graphene nanosheets; GP: graphite powder; I: ionophore; IFS: inner-filling solution; KTFPB: potassium tetrakis[3,5-*bis*(*trifluoromethyl*)*phenyl*]borate; KTpClPB: potassium tetrakis p-(chlorophenyl)borate; LOD: limit of detection; LR: linear range; MWCNT: multi-walled carbon nanotubes; NaTFPB: sodium tetrakis [3,5-bis(trifluoromethyl)phenyl]borate; NaTPB: sodium tetraphenylborate; NGO: graphene oxide nanosheets; NS: not-specified; o-NPOE: 2-nitrophenyl octyl ether; PANI: polianiline; PEDOT: poly(3,4-ethylenedioxythiophene; PO: paraffin oil; POT: poly(3-octylthiophene); PSS^-: polystyrenesulfonate; PVC: polyvinyl chloride; RTIL: room-temperature ionic liquid; SGAN: sol–gel/Au nanoparticle; SSA: 5-sulfosalicylic acid; SS-CPE: solid state carbon paste electrode; SS-CW: solid state coated wire; SS-CP: solid state conductive polymer; TEHP: tris(2-ethylhexyl) phosphate; TPC: 2-thiophenecarboxylic; tr: response time.

provided enhanced sensitivity (reaching a Nernstian response) and higher selectivity over Hg^{2+} (for all other transition metals: $\log K^{pot}_{Ag^+,M^{n+}} < -4.5$) [82]. Of this class of ionophores, the best analytical performances were demonstrated by receptors XIV and XV (Fig. 4). Membranes containing ionophore XIV (1 wt%), PVC (33 wt%) and DOA (66 wt%) provided a LOD of 32 nM and a $\log K^{pot}_{Ag^+,Hg^{2+}} = -4.5$ [71]. Ionophore XV substituted into the same membrane composition resulted in a LOD of 0.8 nM and a $\log K^{pot}_{Ag^+,Hg^{2+}} = -3.3$ [82]. These are not the only non-macrocyclic compounds to have shown good analytical performances; for example, a LOD of 50 nM and a $\log K^{pot}_{Ag^+,Hg^{2+}} = -2.8$ calculated with the fixed interference method (FIM) were achieved using N,N'-bis(benzophenone imine)formamidine, although in this case selectivity towards other ions was inferior to the above-discussed ionophores($\log K^{pot}_{Ag^+,M^{n+}} = -3.0$ (Cu^{2+}) and –2.7 (Pb^{2+})) [27].

Importantly, some bifunctional receptors may act as ionophore for both Ag^+ and perchlorate ions, depending on the ion exchanger included in the membrane. This is the case for a new family of porphyrin dimers synthesized by Lisak et al., which acted as Ag^+ ionophores in the presence of KTClPB and as perchlorate receptors with tridodecylmethylammonium chloride (TDMACl) ion exchanger [25]. The observed dualism was judged to be due to the use of mixed porphyrin dimers containing one anion- and one cation-sensitive porphyrin environment (metalloporphyrin and freebase units, respectively). Interestingly, mixed porphyrin dimers resulted in better selectivity toward Ag^+ than dimers based on two freebase units (*i.e.* $\log K^{pot}_{Ag^+,M^{n+}} = -4.92$ for Na^+ and –2.74 for K^+ with two freebases and $\log K^{pot}_{Ag^+,M^{n+}} = -6.25$ for Na^+ and –4.14 for K^+ using the mixed dimer). However, selectivity against mercury was not reported. More recently, Bobacka et al. found that ISEs based on complexes of rare earth elements with “double-decker” type porphyrins showed impressive selectivity towards Ag^+, especially those containing terbium and yttrium ($Tb^{III}(TPP)_2$ and $Y^{III}(TPP)_2$) [83]. The observed LODs were rather high (between 8 and 10 μM for all the tested ionophores), but this work demonstrated the potential benefits of using density functional theory (DFT) calculations in designing new Ag^+ ionophores, which provided good correlation with the empirically determined selectivity patterns.

Although for ISEs ionophores are usually added directly to the membrane cocktail, grafting onto nanomaterials (either organic or inorganic) has also been reported as an effective strategy for Ag^+ recognition [75]. Since covalent immobilization leads to lower diffusion of ionophores, leaching of membrane components is significantly reduced, resulting in improved durability of the developed ISEs. The group of Gyurcsanyi introduced ionophore - gold nanoparticle conjugates (IP-AuNP), which were based on the spontaneous self-assembly of Ag^+ with thiacalixarene derivatives on the surface of gold nanoparticles [75]. IP–AuNPs were included in a cocktail membrane containing PVC, o-NPOE (ratio 2:1) and NaTFPB. Selectivity coefficients ($\log K^{pot}_{Ag^+,M^{n+}} = -7.4$ for Mg^{2+}, –6.6 for Pb^{2+}, –4.9 for K^+ and –5.7 for Na^+) were higher than those observed with the free ionophore in the membrane ($\log K^{pot}_{Ag^+,M^{n+}} = -11.6$ for Mg^{2+}, –10.8 for Pb^{2+}, –8.4 for K^+ and –10.8 for Na^+), which was attributed to a lower stability of the Ionophore–AuNP–silver complex. Nevertheless, the use of IP–AuNPs provided a LOD of 5 nM, shorter conditioning time, drift-free potential response, and suppression of super-Nernstian behavior at lower Ag^+ concentrations. The same group further explored ionophore grafting onto gold nanopores as a synthetic version of biological ion channels [84]. In this case, all active compounds were covalently grafted to the internal surface area of gold nanopores and a perfluorinated thiol derivative was used to confer hydrophobicity, reaching a LOD of 6.8 nM. Fullerene has also been reported as a nanomaterial that can improve selectivity for silver, especially over mercury, given its large number of π-electrons [74]. The resulting sensor provided a LOD of 0.1 μM and a $\log K^{pot}_{Ag^+,M^{n+}} < -4.2$ for all tested ions, including Hg^{2+}.

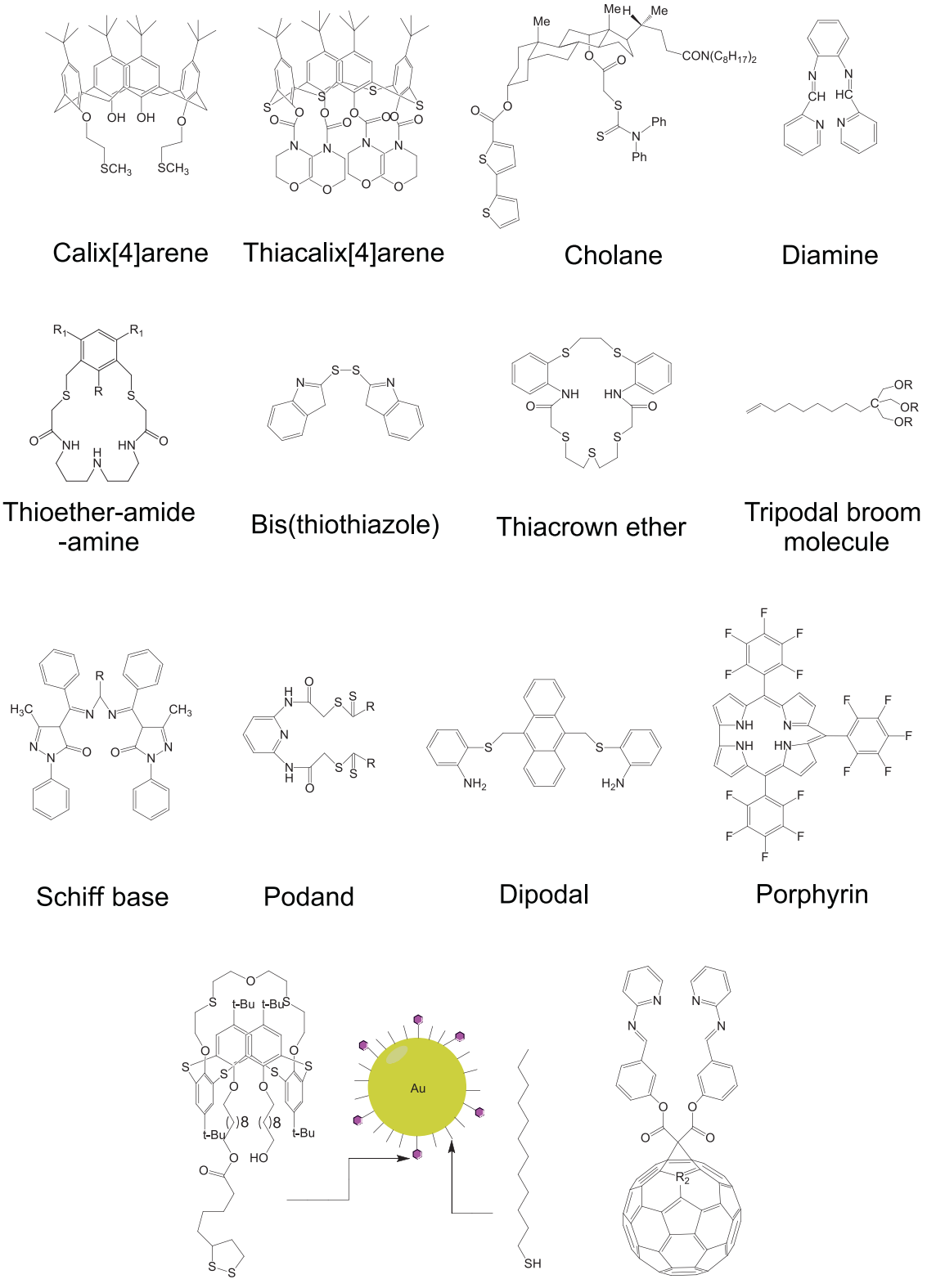

Fig. 1. Representative examples of family compounds commonly employed as silver ionophores.

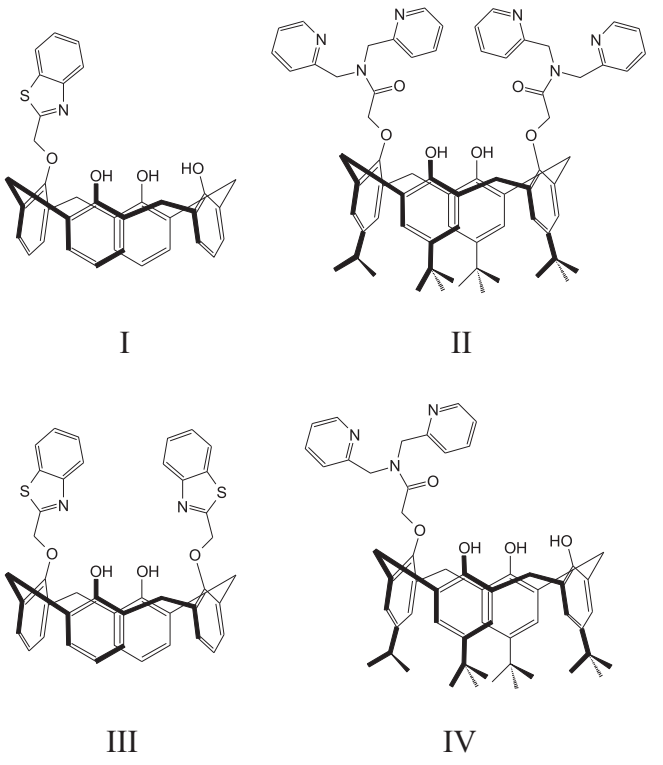

Fig. 2. Four calix[4]arene derivatives reported by Janrungroatsakul et al. as Ag^+ ionophores [77]. One or two opposite phenolic groups of calix[4]arene are modified by either benzothiazole or dipicolylamine.

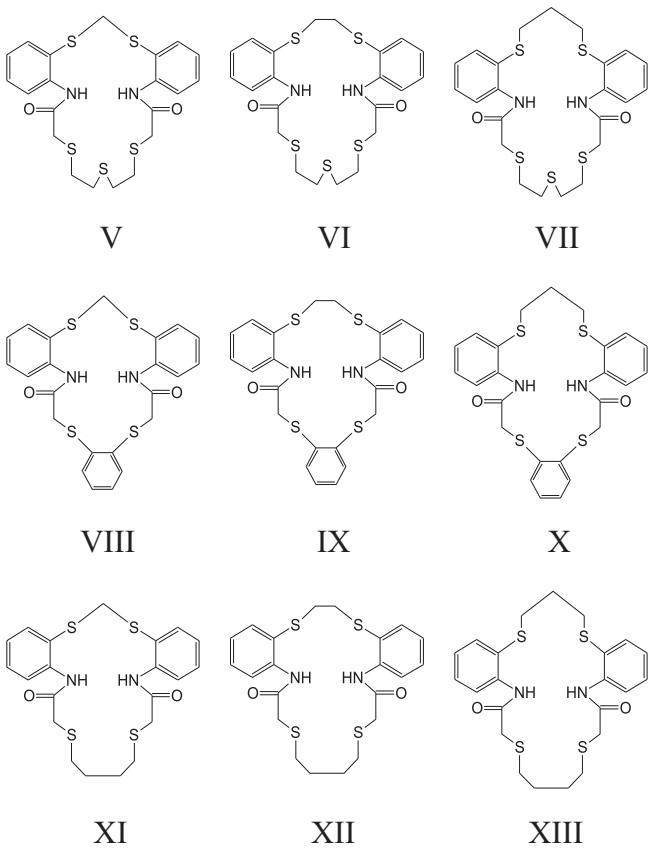

Fig. 3. Nine monoazathiacrown ethers reported by Zhang et al. as Ag^+ ionophores [80] with different ring number and number of sulfur atoms.

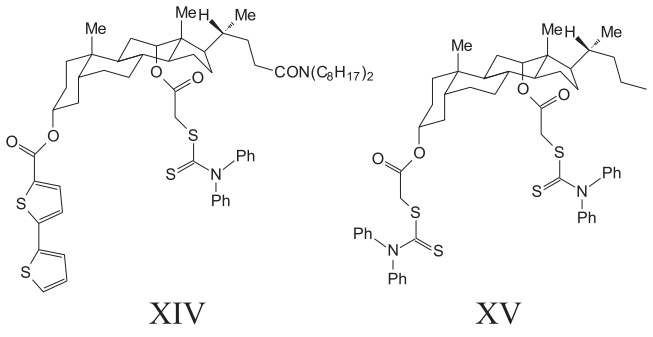

Fig. 4. Cholan-24-amide (N) and cholane (O) derivative synthetized by Kim, Nam and coworkers as Ag^+ ionophores [71,82].

An important development which ought not to be omitted is the use of fluorous sensing membranes, which has been demonstrated to enhance selectivity and LOD of silver-selective electrodes [62,85]. Fluorous membranes contain a high fluorine content, and thereby present non-coordinating and poorly solvating properties. This promotes stronger binding between Ag^+ and the ionophore, and additionally results in weak solvation of interfering ions in the sensing membrane, thus improving electrode selectivity. Using this approach, Lai et al. developed an ISE composed of perfluoro-saturated polymer with 1,3-bis(perfluorodecylethylthiomethyl)benzene as ionophore and three dimensionally ordered macroporous (3DOM) carbon as the solid contact [62]. This approach provided a LOD of 0.38 pM and a remarkably selectivity over sodium (*e.g.* $\log K^{pot}_{Ag^+,Na^+} = -12.9$). However, the electrode presented a very narrow LRR, from 0.1 to 1 nM.

Conventional knowledge regarding silver-selective electrodes targets Hg^{2+} as the most relevant interfering ion. However, mercury levels in the environment have been significantly reduced in recent years due to much stricter regulations on its use [86,87]. As a consequence, environmental Hg^{2+} concentrations are now generally lower than those of Ag^+, suggesting that high discrimination (*i.e.* large selectivity coefficient $\log K^{pot}_{Ag^+,Hg2+}$) is no longer essential. In contrast, selectivity with regards to Na^+ should be carefully evaluated due to the near ubiquitous nature of this ion. For example, in drinking water, the sodium concentration can vary between 43.5 µM and 17.5 mM [88] whereas recommended maximum levels for Ag^+ are 0.92 µM [33]; thus, $\log K^{pot}_{Ag^+,Na^+}$ of at least −3.9 is required to assure accurate Ag^+ measurements in drinking water. Additionally, even better selectivity is necessary for analysis of seawater, which contains about 0.5 M NaCl [89]. From the values of $\log K^{pot}_{Ag^+,Na^+}$ shown in Table 2, it can be observed that only about half of the reported inner-filling solution ISEs for Ag^+ present sufficient selectivity to meet these requirements for Ag^+ detection in environmental waters.

Tighter control of ion fluxes across any membrane interface has been demonstrated to be a crucial factor in determining the LOD associated with Ag^+ selective electrodes [90]. Using low amounts of ion-exchanger and ionophore in the membrane was shown to reduce ion fluxes across membrane interface, whereas loading the membrane with a certain amount of the primary ion salt helps to minimize co-extraction effects [91]. It is essential to reduce the concentration of free Ag^+ in the inner filling solution. In this context, Kim et al. were able to decrease the LOD from 63 nM to 1 nM by adding Na_2EDTA to the inner filling solution [82]. Other methods include actively controlling the ion transport by current or potential [92], the use of polymeric microspheres to suppress the mobility of ions in the membrane [93], the use of methyl methacrylate and decyl methacrylate (MMA-DMA) copolymers to fine-tune

diffusion coefficients, and increasing the membrane thickness [94]. In combination, several strategies aiming to reduce ion fluxes across the membrane can induce a significant decrease of the LOD of ISEs for Ag^+, from micromolar to even subnanomolar levels. Moreover, it has also been reported that these strategies can lead to an improvement in selectivity for silver ions [91]. For example, a classical conditioning in 5 mM $AgNO_3$ solution for the membrane based on S,S-methylenebis(diisobutyldithiocarbamate) results in non-Nernstian slopes and $\log K^{pot}_{Ag^+,M^{n+}}$ between −3.0 and −4.6 for Na^+, K^+, Ca^{2+}, Pb^{2+} and Cu^{2+}, whereas the same electrode conditioned in 10 mM NaCl (thus avoiding prior contact to Ag^+) provides not only Nernstian response to Ag^+ but also near-Nernstian response for all other ions tested (58.7, 59.2 mV dec^{-1} for Na^+, K^+, 25.3, 35, 32 mV dec^{-1} for Ca^{2+}, Pb^{2+}, Cu^{2+}, respectively), with $\log K^{pot}_{Ag^+,M^{n+}}$ between −8.2 and −11.0 for all these ions, almost three times lower than the values obtained with the classical conditioning protocol [95].

A particular case of potentiometry that allows for a better control of ion fluxes across the membrane is the use of galvanostatic pulse chronopotentiometry (also known as pulstrode) [92,96]. This measurement protocol consists of a sequence of three steps: (i) determination of open circuit potential (OCP) at zero-current conditions; (ii) galvanostatic interrogation pulse; and (iii) application of a potential equal to the OCP. Specifically, the galvanostatic pulse induces an ion-exchange process whereby electrolytes are extracted from the sample into the membrane (this process is assisted by the ionophore in case of the primary ion) and counterions are extracted from the inner solution of the electrode to maintain electroneutrality in the entire system [97]. This pulse results in a potential decay, with the endpoint considered to be the potential signal of the ISE, exhibiting a near-Nernstian response in total analogy to zero-current potentiometry. Finally, the application of a potential equal to the initial OCP of the electrode permits the regeneration of the membrane and, therefore, the generation of reproducible signals [98]. Because the ion-exchange process is controlled by the applied galvanostatic pulse, there is no ion-exchanger in the membranes in pulstrodes. Therefore counter-transport affects are avoided, and this facilitates Nernstian response to any ion (primary and interferences). Furthermore, the total ion exhaustion, enforced by the OCP potential pulse, has been demonstrated to lead to unbiased selectivity coefficients [99]. A very interesting Ag^+ pulstrode was reported by Makarychev-Mikhailov et al. based on a silver-selective membrane containing bis-thioether functionalized *tert*butyl calix[4]arene as ionophore [96]. The resulting LRR was narrower than that provided by conventional ISEs (*i.e.* about one activity decade), but this range could be tuned in principle by varying the magnitude and duration of the galvanostatic pulse. Thus, the pulstrode was able to detect Ag^+ with concentrations in the range from less than 10^{-7} M to more than 10^{-4} M. A clear advantage of pulstrodes is that the observed potentials are independent of the reference electrode, opening a new perspective into the miniaturization of sensors [96].

The all-solid-state concept was conceived to solve a series of drawbacks related to the presence of the inner-filling solution in ISEs, including the suppression of ion-fluxes at the internal membrane interface [100]. This configuration also furnishes ISEs with a versatility for adaptation in miniaturized and differently shaped electrode platforms [101]. The all-solid-state silver-selective electrodes reported in the literature over the last decade tend to come in the form of coated wire electrodes or carbon paste electrodes, and generally use conducting polymers as the ion-to-electron transducer (see Table 2). The few coated wire ISEs for Ag^+ presented LODs at the micromolar level, and rather unsuitable selectivity towards sodium (*e.g.*, $-4 < \log K^{pot}_{Ag^+,Na^+} < -0.5$) [102-104], showing therefore a limited analytical performance comparable to the classical inner-filling solution ISEs. Furthermore, coated wire ISEs are known to provide unstable response due to the low capacitance at the metal-membrane interface and lack of a well-defined ion-to-electron transducer [105].

Different kinds of conducting polymers have been reported as effective ion-to-electron transducers in ISEs for Ag^+. Lisak et al. presented a glassy carbon electrode (GCE) modified with electropolymerized poly(3,4-ethylenedioxythiophene) (PEDOT) doped with polystyrenesulfonate [25], presenting LODs between 10 and 20 µM. Yin et al., presented Ag^+ detection with an electrode prepared with poly(3-octylthiophene) (POT) as the transducer and a membrane based on o-xylylene-bis(N, Ndiisobutyldithiocarbamate) as ionophore [106]. In this case, POT was directly mixed with the membrane cocktail, thereby constituting a single-piece solid-contact ISE. The LOD achieved with the resulting electrode was 19 nM. ISEs for Ag^+ based on POT were also reported by Woznica et al., particularly using gold NPs to anchor the ionophore within the membrane phase [107]. This strategy provided an improvement in the upper detection limit, allowing a Nernstian response to be maintained up to 0.1 M Ag^+. However, such high concentrations of silver are unlikely to occur in any real sample. Besides PEDOT and POT, other conducting polymers employed for silver-selective electrodes include polyaniline (PANI) [108] and polypyrrole [109].

Interestingly, the majority of all-solid-state ISEs for Ag^+ reported in the last decade are based on carbon paste, which can act as both electro-conductive material and Ag^+ receptor. In a study using the former option, with deposition of the ion-selective membrane on top [110], the LRR for Ag^+ detection was found to be between 10^{-5} and 10^{-1} M. However, much lower LODs (between 10 and 100 nM) were claimed when the carbon paste acts as both electro-conductive material and Ag^+ receptor [27,111,112]. In this type of electrode, the carbon paste usually contains graphite powder (30 – 70 wt%), paraffin oil (20 – 40 wt%) and Ag^+ ionophore (1 – 10 wt%), and no polymer substrate is incorporated. Afkhami et al. developed a carbon paste electrode (CPE) based on the addition of graphene nanosheets and diphenylacetylene (DPA, a conductive binder agent) onto the carbon paste containing thionine as Ag^+ ionophore [26]. The incorporation of graphene nanosheets seemingly provided enhanced conductivity and a larger surface area, whereas the replacement of paraffin oil by DPA resulted in a higher sensitivity due to its $\pi - \pi$ interactions with graphene. Overall, the analytical performance was significantly improved as compared to the unmodified CPE, achieving a LOD of 4.2 nM and a LRR from 8 nM to 10 mM. In another study, Yang et al. grafted the ionophore 2-thiophenecarboxylic acid onto graphene and decorated it with gold nanoparticles (AuNPs) [113]. This provided a hybrid nanomaterial that acted as both receptor and ion-to-electron transducer which was able to overcome problems associated to the leaching of membrane components. Beyond graphene, carbon nanotubes are another popular carbon nanomaterial that has displayed improved analytical performance of ISEs for Ag^+ [111,114,115].

AuNPs have additionally demonstrated suitability in improving the electron-transfer process between the electrode surface and the electrolyte [112,116]. Ramenazi et al. reported a CPE comprising Schiff base N,N'-di-(cyclopentadienecarbaldehyde)−1,2-di(o-aminophenylthio)-ethane as ionophore and encapsulated AuNPs in a 3-(mercaptopropyl)-trimethoxysilane (MPTS) derived sol-gel network [112]. The encapsulation of AuNPs was achieved *via* S-Au covalent bonding and provided high electrical conductivity and an increased surface area along the three-dimensional electrode. Electrical conductivity and long-term stability were further improved by the substitution of paraffin oil by room-temperature ionic liquids, giving rise to higher sensitivity and lower response time [112]. The resulting sensor provided a LOD of 0.8 nM and a LRR from 2.4 nM to 22 mM, with a fast response time (5 s) and adequate selectivity over sodium ($\log K^{pot}_{Ag^+,Na^+} = -5.5$).

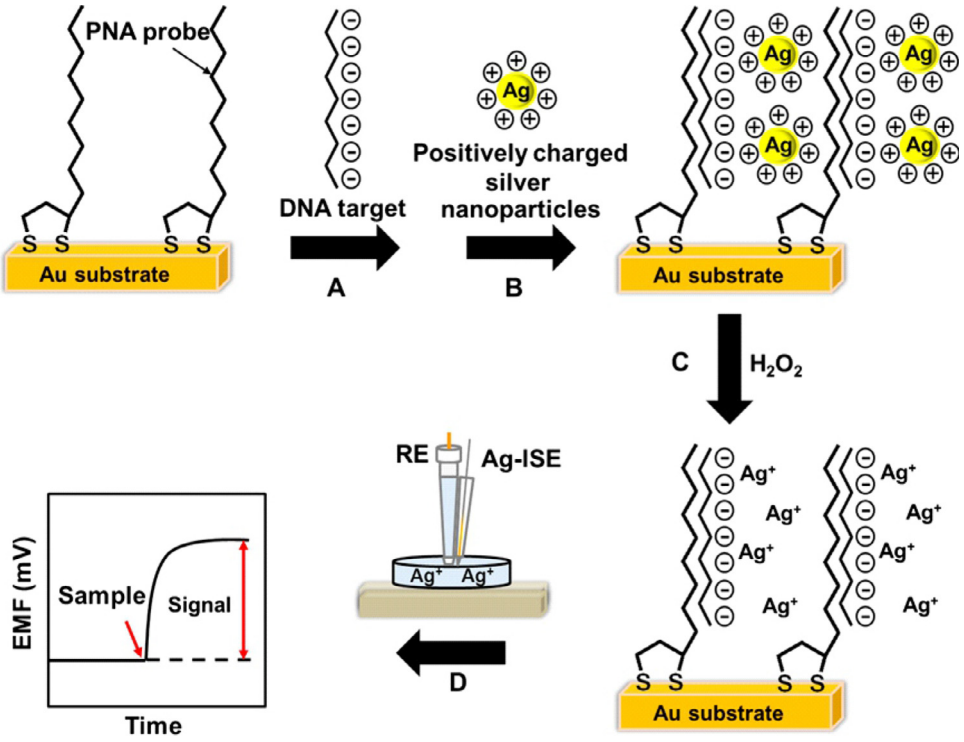

Fig. 5. Representation of the sensing mechanism for the AgNPsþ-based label-free potentiometric DNA detection reported by Janrungroatsakul et al. Reproduced with permission from ref. [77].

While inner-filling solution electrodes were primarily demonstrated for halide titrations and the determination of samples containing high silver contents (*e.g.* photographic and radiological films, or spiked water samples) [57,72], the all-solid-state concept opened up new applications such as on-site water analysis [19,23], AgNPs speciation [117] and the use of silver as an indirect marker to study protein interactions [44]. These new applications are possible not only because of the improved analytical performance of all-solid-state ISEs but also because the removal of the inner-filling solution facilitates electrode miniaturization, and thereby decentralized silver measurements. Moreover, the use of inner-filling solution ISEs represents a challenge for *in situ* water analysis, because inner-filling solutions are susceptible to evaporation and highly sensitive to changes in temperature and/or pressure [19]. Unfortunately, the vast majority of the papers published on the last decade about silver-selective electrodes show a focus on the search for improved analytical performance of ISEs, without much exploration of their potential applications. It is common to find lab-bench applications that consider relatively high levels of Ag^+ and, particularly, spiked samples. Also, on many occasions, complex sample pre-treatments such as acid digestion [112], filtration [60] and dry ash in muffle furnaces [118] are required. The need for such complex experimental procedures also impedes decentralized measurements.

Janrungroatsakul et al. applied silver-selective electrodes based on calix[4]arene derivatives to the detection of DNA hybridization [77]. A peptide nucleic acid DNA probe was covalently attached to a gold substrate. Then, hybridization of target DNA resulted in a negatively charged surface that was used to adsorb positively charged AgNPs. These AgNPs were subsequently oxidized with hydrogen peroxide to release Ag^+, which was detected by a silver-selective electrode. The sensing mechanism is illustrated in Fig. 5. This method allowed for the discrimination of fully complementary DNA from single base mismatched and non-complementary DNA, achieving a LOD for DNA of 0.2 µM. A similar approach was also used for glucose sensing [74,119]. In this case, the oxidation of glucose by the glucose oxidase enzyme generates hydrogen peroxide, which oxidizes AgNPs to Ag^+. In fact, this procedure allows speciation analysis to differentiate between Ag^+ and AgNPs in a two-step measurement protocol: initial Ag^+ detection followed by total silver analysis after complete oxidation of AgNPs to Ag^+ (quantity of AgNPs is therefore calculated as the difference between the two measurements) [120].

Bobacka et al. have recently investigated the spontaneous and stimulated dissolution of AgNPs in real time using an all-solid-state silver-selective electrode comprising o-xylylenebis(N,N-di*iso*butyldithiocarbamate as Ag^+ ionophore and mesoporous carbon as solid contact [117]. Kinetic assessment carried out by this ISE for 8 h showed comparable results to discrete measurements by ICP-MS, with the advantage of providing real time, continuous information with the ISE. Speciation of silver between Ag^+ and AgNPs, was possible because potentiometric ISEs provide information about ion activity (*i.e.* effective concentration of a species in a non-ideal solution) rather than total concentration. Thus, ISEs discriminate free Ag^+ from other silver species (complexes and nanomaterials), which is very useful in both clinical and environmental fields given that free silver ions are the main agent responsible for physiological and toxicological effects.

3. Voltammetric determination of silver

Table 3 summarizes the most relevant voltammetric sensors reported in the last decade for the determination of silver, focusing on: the type of electrode, the silver species determined, the type of voltammetric technique, and the main analytical parameters (LOD and LRR). In addition, the electrochemical protocol and the analytical application are collected in Table 3, aiming to provide a more thorough assessment of the potential of each reported sensor for application in decentralized analysis. Notably, the electrochemical protocol most widely used is stripping voltammetry after the

Table 3
Silver determination by stripping voltammetry.

Electrode	Analyte	Technique	Accumulation step	LOD	LRR	Application	Ref
GaN micropillars	Ag^+	DPASV	$E_d = -0.1$ V, $t_d = 180$ s	30 nM	93 nM – 9.3 μM	Tries tap water but levels are too low	[28]
Graphite electrode impregnate with polyethylene	Ag^+	LSASV	$E_d = -0.7$ V, $t_d = 120$ s (vibration)	0.15 μM	0.15 – 46 μM	Standard samples of Cu and Ni sludge and pyrite from the Kirovsko-Kryklyns kaya ore zone	[177]
Boron doped diamond, disk and planar	Ag^+	DPASV	$E_d = -0.3$ V, $t_d = 120$ s	6.5 nM (disk) 16 nM (planar)	9.3 – 690 nM (disk) 46 nM – 2.3 μM (planar)	Water reference solution (NIST) and simulated ISS potable water (NASA)	[157]
CPE or SPCE modified with chromium oxide	Ag^+	SWASV	$E_d = -1.3$ V, $t_d = 100$ s	28 nM	93 nM – 4.6 μM	Industrial water but does not find silver	[193]
Porous GaN	Ag^+	SWASV	$E_d = -0.5$ V, $t_d = 120$ s	4.6 nM	9.3 – 930 nM	None	[132]
Conductive hybrid diamond/graphite film	Ag^+	DPASV	$E_d = -0.1$ V, $t_d = 180$ s	54 nM	93 nM – 930 μM	Spiked tap water	[158]
CPE modified with silver IIP	Ag^+	DPASV	$E_d = -0.4$ V, $t_d = 180$ s	0.11 nM	0.5 nM – 0.28 μM	Certified reference material and spiked tap, river and groundwater	[194]
Graphite felt	Ag^+	DPASV	$E_d = -0.6$ V, $t_d = 90$ s	25 nM	27 nM – 1.6 μM	None	[31]
Wurtzite GaN	Ag^+	DPASV	$E_d = 0$ V, $t_d = 180$ s	65 nM	0.46 – 9.3 μM	None	[159]
Nanocrystalline cubic SiC thin film	Ag^+	DPASV	$E_d = 0$ V, $t_d = 180$ s	37 nM	93 nM – 9.3 μM	None	[160]
CPE modified with CNT	Ag^+	DPASV	$E_d = -0.4$ V, $t_d = 120$ s	1.8 nM	10 – 1000 nM	Spiked sea, mineral and well water	[156]
GCE	Ag^+ in the presence of AgNP	SWASV	$E_d = -0.5$ V, $t_d = 120$ s	12 nM	23 – 180 nM	Commercial products of colloidal silver	[178]
In-situ bismuth film on GCE	Ag^+ in the presence of AgNP	SWASV	$E_d = -0.8$ V, $t_d = 60$ s	19 nM	93 – 830 nM	Supernatant of a commercial AgNP suspension	[155]
Au and Pt micro and nanoelectrodes	Ag^+	ASV	$E_d = -0.3$ V, $t_d = 60$ s (micro), $t_d = 30$ s (nano)	1.3 pM	1.3 – 80 nM	None	[162]
GCE coated with LB film containing polyaniline doped with PTSA	Ag^+	LSASV	$E_d = -0.56$ V, $t_d = 200$ s	0.4 nM	0.6 nM – 1 μM	Spiked tap and lake water	[195]
GCE modified with N-(2-aminoethyl)−4,4′-bipyridine	Ag^+	DPASV	$E_d = -0.6$ V, $t_d = 180$ s	25 nM	50 – 1000 nM	Spiked river and tap water	[134]
CPE modified with bis(2-hydroxyaceto phenone) butane-2,3-dihydrazone	Ag^+	DPASV	$E_d = -0.9$ V, $t_d = 300$ s	6.7 nM	10 nM – 2 μM	X-ray photographic film and spiked spring water	[137]
CPE modified with poly(methylene disulfide) NP	Ag^+	DPASV	$E_d = -0.3$ V, $t_d = 480$ s	0.1 pM	3 pM – 1 nM	Spiked tap and river waters and tea leaves	[29]
CPE modified with 2-hydroxybenzaldehyde	Ag^+	DPASV	Accumulation at OCP for 3 min followed by Ag^+ reduction at 0 V for 3 min	9.3 pM	9.3 pM – 0.93 μM	Certified reference estuarine water and river water	[30]
CPE modified with AuNPs and DNA probes	Ag^+	DPV	DNA hybridization at 0.5 V for 5 min followed by immobilization of label for 5 min at OCP	24 pM	90 pM – 1 nM	Spiked tap, river and sea water	[144]
GCE modified with GOx	Ag^+	Amperometry	None	1.8 nM	20 – 200 nM	None	[172]
CPE modified with silver-chelating Schiff base	Ag^+	DPASV	Accumulation at OCP for 12 min followed by Ag^+ reduction at −0.7 V for 20 s	0.74 nM	4.6 nM – 2.2 μM	Photographic films and spiked tap, well and wastewater	[145]
CPE modified with p-isopropylcalix[6]arene	Ag^+	DPASV	Accumulation at OCP for 3 min followed by Ag^+ reduction at −0.25 V for 35 s	48 nM	50 nM – 2 μM	X-ray photographic film	[165]
CPE modified with Schiff base of N,N'-bis (2-hydroxybenzylidene)−2,20 (aminophenylthio) ethane	Ag^+	DPASV	Accumulation at OCP for 9 min followed by Ag^+ reduction at −0.7 V for 20 s	0.85 nM	4.6 nM – 1.8 μM	X-ray photographic films and spiked tap, well and Persian gulf water	[164]
GCE modified with 4-tert-butyl-1-(ethoxy carbonyl-methoxy)thiacalix[4]arene	Ag^+	DPASV	Accumulation at OCP for 20 min followed by Ag^+ reduction at −0.6 V for 30 s	10 nM	50 nM – 3 μM	Spiked tap, lake and synthetic water	[133]
CPE modified with DNA probe	Ag^+	DPV	Incubation for 600 s	10 pM	20 pM – 1 nM	Spiked tap water and dental amalgam	[168]

(*continued on next page*)

Table 3 (*continued*)

Electrode	Analyte	Technique	Accumulation step	LOD	LRR	Application	Ref
CPE combined with magnetic silver IIP NPs	Ag^+	DPASV	Incubation for 4 min with NPs followed by Ag^+ reduction at -0.8 V for 40 s	0.14 nM	0.46 nM – 1.4 μM	Spiked dam, aqueduct and well water	[166]
Carbon ceramic electrode modified with 4-(2-pyridylazo)-resorcinol	Ag^+	DPASV	Accumulation at OCP for 12 min followed by Ag^+ reduction at −0.6 V for 15 s	1.1 nM	4.6 nM – 2.8 μM	X-ray photographic films and super-alloy samples	[163]
AuE modified with sulfur QDs	Ag^+	DPV	NS	71 pM	0.1 nM – 3 mM	Spiked tap and pond water	[136]
AuE modified with 16-mercaptohexadecanoic acid	Ag^+	DPV	Incubation with C-rich ssDNA for 10 min and MWCNT for 15 min followed by deposition on electrode and drying for 80 min	1.3 nM	10 – 500 nM	Spiked lake and river water	[169]
AuE modified with DNA probes containing adenine and cytosine	Ag^+	ACV	None	9.3 nM	9.3 – 93 nM	Spiked synthetic human saliva and silver sulfadiazine	[135]
AuE modified with GOx	Ag^+	Amperometry	None	2 nM	2 – 40 nM	Spiked tap, spring and river water	[171]
Edge plane ordinary pyrolytic graphite	Ag^+	DPV	Precipitation with NaCl for 4 min followed by reduction at −0.7 V for 60 s	235 μM	NS	None	[138]
Pyrolytic graphite electrode	Ag^+	DPASV	Evaporation of solvent for 4 min during AgCl precipitation followed by Ag^+ reduction at -0.39 V for 15 s	0.19 μM	0.56 – 92 μM	None	[139]
Magnetic GCE	Ag^+	DPV	Incubation for 5 min with NPs followed by Ag^+ reduction at −0.5 V for 120 s	3.3 nM	0.12 – 18 μM	Spiked tap, lake and synthetic water	[167]
MWCNT modified GCE	Ag^+	DPASV	Incubation with guanine for 20 min followed by Ag^+ reduction at 0.3 V for 240 s	30 nM	0.1 – 2.5 μM	Spiked pond and well water	[170]
GCE modified with POT and thin-layer polymeric membrane	Ag^+	ALSV	E_{acc} = 0 V, t_{acc} = 720 s	5 nM	5 – 100 nM	Spiked water samples	[24]
GCE modified with POT and thin-layer polymeric membrane	Ag^+	ALSV	E_{acc} = 0 V, t_{acc} = 1440 s	0.05 nM	0.05 – 10 nM	Spiked water samples	[173]
GCE modified with L-lysine	Ag^+, AgNP	DPV	Drop-casted onto WE and dried with N_2	93 pM	0.18 – 93 nM	Ionic and colloidal silver commercial antibiotic	[179]
CPE modified with poly(4-vinylpyridine) or Fe(II,III) oxide	AgNP	DPV	Rotating electrode for 2–24 h in solution	< 9.2 nM	NS	Spiked lake, mineral and wastewater	[183]
SPCE	AgNP	LSV	Drop-casted onto WE and dried with N_2	NS	NS	Commercial colloidal products	[184]
SPCE modified with cysteine	AgNP	LSV	Immersion from 0 to 960 min	NS	NS	Spiked sea water	[180]
AuE modified with DMSA	AgNP	ASV	Immersion at OCP from 3 h to 96 h	NS	NS	None	[181]
GCE	AgNW	LSV	Adsoption without potential for 10 min	32 pM	46 pM – 23 nM	Wastewater from AgNW film preparation and spiked tap water	[192]

ACV: alternating current voltammetry; ALSV: anodic linear sweep voltammetry; AuE: gold electrode; CPE: carbon paste electrode; DPASV: differential pulse anodic stripping voltammetry; DPV: differential pulse voltammetry; GCE: glassy carbon electrode; GOx: glucose oxidase; IIP: ion imprinted polymer; LB: Langmuir–Blodgett; LSASV: linear sweep anodic stripping voltammetry; LSV: linear sweep voltammetry; NP: nanoparticle; NS: not specified; NW: nanowire; OCP: open circuit potential; PTSA: p-toluenesulfonic acid; QD: quantum dot; SPCE: screen-printed carbon electrode; SWASV: square wave anodic stripping voltammetry.

pertinent accumulation step. Indeed, a key aspect in lowering the LOD and achieving the determination of trace levels of silver is an appropriate optimization of the accumulation step.

Several strategies are available for this purpose, with the most common illustrated in Fig. 6. The first strategy (Fig. 6a) corresponds to the classical approach of anodic stripping voltammetry (ASV) which is the preferred technique for metal and carbon-based electrodes. Initially, a negative deposition potential (E_d, usually between –0.7 V and 0 V) is applied for a given deposition time (t_d, usually between 60 and 180 s) to reduce Ag^+ to metallic silver, which is accumulated on the electrode surface. Afterwards, during the stripping step, metallic silver is re-oxidized back to Ag^+ and released from the electrode surface, giving rise to an oxidation peak. Thus, the analytical performance is highly dependent on the electrode material, with the lowest reported LOD in the order of nanomolar levels and the widest LRR covering two orders of concentration magnitude [28,31,132].

The second strategy for the accumulation step (Fig. 6b) is exclusive to electrodes modified with a ligand that presents affinity for silver (*e.g.* calixarenes [133], bipyridines [134], DNA probes [135]). Immersion of the electrode in the sample at the OCP allows for the binding of Ag^+, being directly accumulated at the electrode sur-

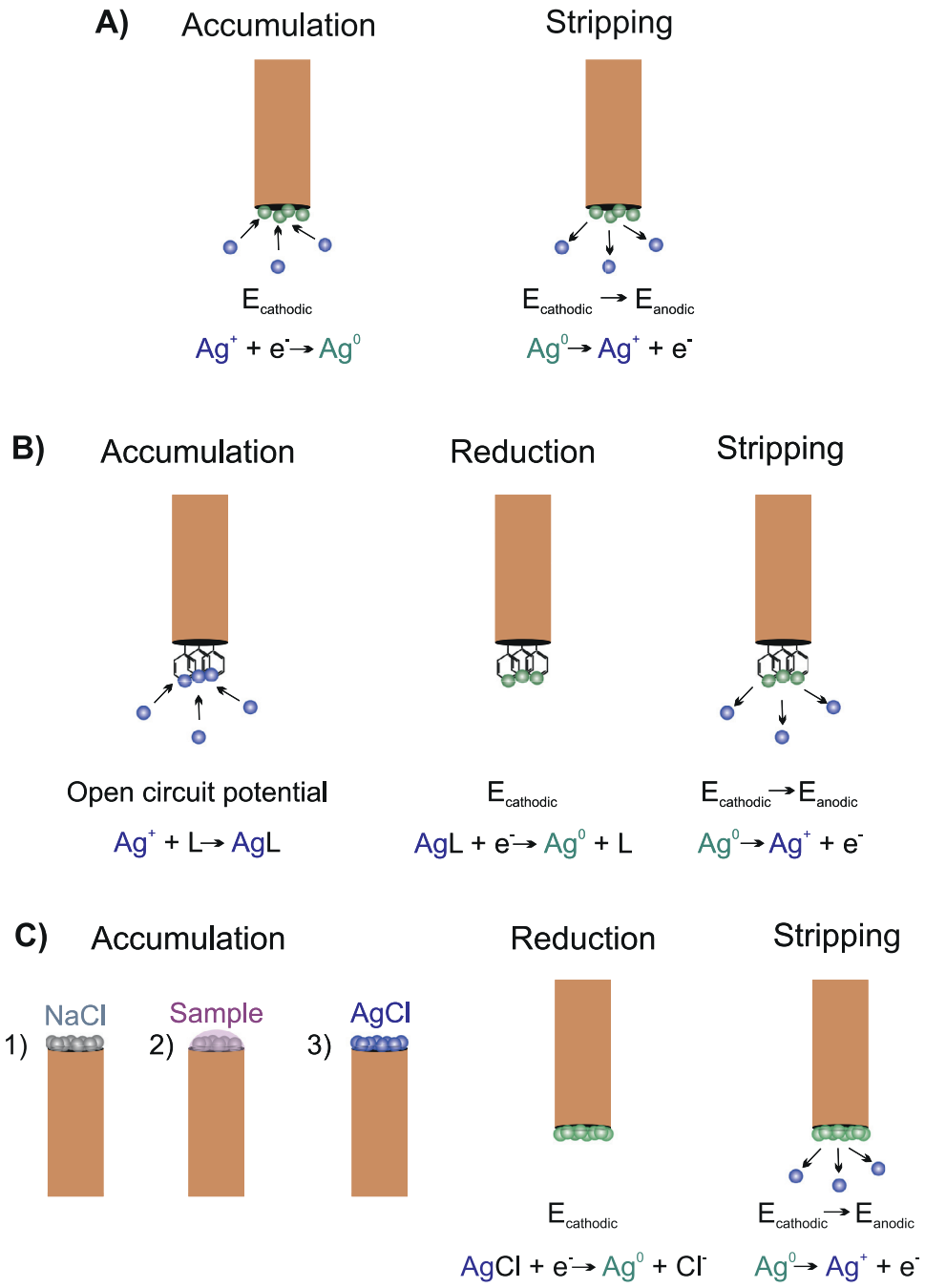

Fig. 6. Accumulation strategies reported for the stripping voltammetric determination of Ag^+. a) Traditional ASV method, b) Accumulation based on ligand-silver binding, c) Stripping voltammetry microprobe.

face. This step is traditionally followed by the application of a negative potential that reduces the accumulated Ag^+ to metallic silver, which is then re-oxidized back during the stripping step. This latter results in an oxidation peak, which is usually better defined than a reduction peak. Although the deposition step is usually longer (3 – 20 min), in many cases, this second strategy displays significantly improved analytical performance compared to traditional ASV, lowering the LOD to subnanomolar levels and slightly widening the LRR [30,136]. Evidently, a crucial aspect here is the selection of the ligand: binding must be strong enough to accumulate Ag^+, but not too strong to prevent release during oxidation and/or the stripping step. As metal-ligand bonds are strongly influenced by pH, the binding and unbinding of Ag^+ is usually controlled by carefully optimizing both the accumulation and the stripping media. Indeed, in many cases, the pH needed for each step is significantly different, which forces the use of two different media. For example, a bis(2-hydroxyacetophenone)butane-2,3-dihydrazone modified CPE reported by Gholivand et al. required 0.1 M $NaNO_3$ during the accumulation of Ag^+ and 5 mM HCl for the stripping step [137].

Despite the two described strategies being the most common in the literature, some authors have also explored other approaches for the accumulation step. Gulppi et al. developed the so-called stripping voltammetry microprobe, a method based on the precipitation of silver chloride allowing for the analysis of low sample volumes (Fig. 6c) [138,139]. Sodium chloride is first adsorbed onto the electrode surface by either cyclic voltammetry or drop-casting. After that, a small volume of the sample containing silver ions

(2–10 µL) is drop-cast onto the electrode surface and the solvent evaporated in the oven under vacuum. This step results in the complete precipitation of silver chloride, which is then reduced back to Ag^0 with the application of a negative potential and re-oxidized to Ag^+ during the stripping step. In this case, the LOD and the LRR were found to depend on the electrolyte concentration: with higher electrolyte content the LOD decreases and the linearity increases. However, for samples with low silver content ($<10^{-7}$ M), a larger volume is needed, which is not always compatible with electrodes presenting small geometrical area.

Regardless of the strategy used, the accumulation step is always an important factor in lowering the LOD. Nevertheless, this step also represents a challenge for the implementation of stripping voltammetric methods to the on-site determination of silver. First, preconcentration of silver requires an accumulation [140] or deposition time [141-143], which coupled to the time required for the reduction step, can easily result in measurement times of at least 3–5 min. Even longer times are needed to reach subnanomolar levels [144,145]. Thus, real-time monitoring of silver is only possible in those scenarios where silver concentration does not undergo rapid change (*i.e.* high frequency measurements are not required). Second, in most of the reported studies, the accumulation step takes place under magnetically stirred solutions, which cannot really be implemented in most decentralized measurements. This drawback may be overcome by using rotating/vibrating electrodes, although the ensuing change in mass-transport is expected to affect the analytical performance. Particularly interesting is the combination of vibration with microelectrodes, as this lowers the diffusion layer thickness down to ~1 μm, ensuring high mass transport and a low LOD for a short deposition time [146]. Third, complete stripping is required to remove the remaining accumulated metals between measurements and provide good reproducibility [140,147]. In some cases, simple electrochemical protocols based on the application of an oxidative potential for a certain amount of time (30–480 s) in the measuring solution are enough for the same purpose [140]. These protocols are easy to implement in decentralized analysis, although they prolong the analysis time. Sometimes complete stripping is only possible in the presence of oxidative acids (*e.g.* nitric acid, perchloric acid) or strong ligating agents (*e.g.* EDTA) [148], which is not really feasible in on-site analyses. Fourth, accumulation steps based on the formation of a metal-ligand complex are usually dominated by absorption processes. Therefore, keeping the electrode immersed in the sample between measurements may result in extraneous absorption that will therefore provide overestimated results. Furthermore, those methods that require different media for the accumulation and stripping steps are less suitable for decentralized analysis.

3.1. Detection of free Ag^+

Metal ion determination by stripping voltammetry has been historically dominated by the hanging drop mercury electrode (HDME), since polarography was first introduced in 1922 by Heyrovsky [149,150]. The determination of silver at the HDME was not simple to elucidate because silver and mercury present very similar standard reduction potentials (0.799 V for Ag^+/Ag, 0.854 V for Hg^{2+}/Hg, and 0.789 V for $Hg_2{}^{2+}$/Hg), which resulted in the silver signal being masked by the oxidation wave of mercury [151]. This high oxidation potential of Ag^+/Ag not only represents a challenge for the HDME but also for other voltammetric electrodes that have been replacing the HDME in the determination of trace metal ions. This is the case of bismuth and antimony film electrodes [152-154]: a narrow anodic potential window prevents the application of most bismuth and antimony film electrodes to the voltammetric determination of Ag^+, which can only be carried out with *in situ* deposited films as the metallic film is renewed for every measurement. Rominh et al. reported on the *in situ* modification of bismuth on a GCE for the determination of Ag^+ in the presence of oxygen, showing a LOD of 19 nM and LRR of 93–830 nM [155]. *In situ* modified films, however, require the presence of a large concentration of the film metal (*e.g.* 0.5 mg L^{-1} of bismuth reported by Rominh et al. [155]) in the sample solution, which could be inconvenient for decentralized measurements.

The development of voltammetric sensors for the determination of Ag^+ requires the use of electrode materials that are stable at highly positive potentials. Such stability has been provided by carbon electrodes modified with different nanostructures. In this context, the determination of Ag^+ based on the classical approach of ASV has been reported for the CPE modified with CNTs [156], graphite felt electrode [31], boron-doped diamond (BDD) [157] and hybrid diamond/graphite films [158]. Out of these examples, the CNT modification provided the lowest LOD (1.8 nM) [157] whereas the widest LRR was achieved by a planar BDD electrode (46 nM – 2.3 µM) [156]. The potential window was studied in depth by Guo et al., who developed a hybrid diamond/graphite film with a potential window between –1.2 V and 1.9 V, very similar to that observed for BDD and positive enough to allow the determination of Ag^+ [158]. Nevertheless, these carbon-based electrodes require very delicate treatments, and the fabrication process following the published preparation protocols is often highly complicated.

Other, non-carbon-based nanostructured materials have also been reported for the voltammetric determination of Ag^+. One such is gallium nitride (GaN) [28,132,159], a biocompatible semiconductor with excellent chemical stability under harsh conditions that provides low background current and a large potential window suitable for Ag^+ determination. Notably, analytical performance seems to depend on its structure and topology (*e.g.* wurtzite, porous, micropillars), but in all cases the reported LOD was below 70 nM. The lowest LOD was demonstrated by porous GaN, attributed to the higher active area and greater number of binding sites provided by the pores [132]. Hao et al. reported analogous analytical performance (LOD of 37 nM and LRR of 93 nM – 9.3 µM) using cubic silicon carbide (SiC) [160], another semiconductor with high chemical and mechanical stability that offers a potential window of 3.0 V in 0.1 M H_2SO_4 [161]. Even lower LODs were reported by Sidambaram et al. using platinum and gold micro and nanoelectrodes, achieving the lowest LOD (1.3 pM) with a platinum nanoelectrode in 0.1 M chloride-free phosphate buffer [162]. However, the determination of such low Ag^+ concentrations was highly affected by the presence of chloride, which induced the precipitation of silver chloride. This in turn resulted in the anodic stripping peak shifting to less positive potentials, and the appearance of an additional wave that was attributed to silver chloride deposition at the electrode surface.

A second group of electrodes reported for the voltammetric determination of Ag^+ is based on the immobilization onto carbon or gold electrodes of a ligand that presents affinity towards Ag^+. Different compounds have been reported for this purpose, including 2-hydroxybenzaldehyde benzoylhydrazone (2-HBBH) [30], 4-(2-pyridylazo)-resorcinol (PAR) [163], N-(2-aminoethyl)−4,4′-bipyridine (ABP) [134], bis(2-hydroxyacetophenone)butane-2,3-dihydrazone (BHAB) [137], silver-chelating Schiff bases [145,164] and calixarenes [133,165]. Several modification strategies exist for the immobilization of such ligands, including mixing in carbon paste [29,30,137,145,164,165], drop-casting [133], dip-coating [163], or covalent immobilization through aryl diazonium salt electrografting [134]. This type of electrode is compatible with the two main accumulation strategies discussed above (see Fig. 3a and Fig. 3b) and usually provides lower LODs and wider LRRs than electrodes that do not contain any ligand. It seems that the lowest LODs are attained when the accumulation step involves formation of the Ag^+– ligand complex followed by its further reduction.

Gholivand et al. developed a CPE modified with BHAB that, upon application of a conventional ASV deposition protocol with a duration of 300 s, was able to reach a LOD of 6.7 nM and a LRR of 10 nM – 2 μM [137]. El-Mai et al. reported a CPE modified with 2-HBBH with an initial accumulation step at the OCP for 3 min to bind Ag^+ followed by reduction of the complex at 0 V for a further 3 min [30]. Following this strategy, the LOD was as low as 9.3 pM while still offering a wide LRR from 9.3 pM to 0.93 μM. Other examples involve the use of longer accumulation periods (such as 9 and 20 min) [133,164] and present interferences from other ions such as Cu(II), Hg(II), Pb(II) and Cd(II) that can bind the chosen ligand [164].

The combination of nanomaterials and ligand-based electrodes has also been explored. Ghalebi et al. modified a CPE with poly(methylene disulfide) NPs, thus taking advantage of the known affinity between sulfur and Ag^+ [29]. Sensitivity towards silver, deemed as a soft cation, is significantly improved by the inclusion of this soft ligand in comparison to the non-modified (bare) CPE; following a traditional ASV deposition with 480 s, the LOD and LRR obtained were indeed found to be excellent at 0.1 pM and 3 pM – 1 nM, respectively. Fu et al. also exploited S-Ag^+ interactions to develop a sulfur quantum dot (SQD) modified gold electrode with LOD of 71 pM and a very wide LRR from 0.1 nM to 3 mM [136]. Given the non-conductive nature of SQD, the amount deposited onto the electrode surface shows a great influence in the resulting analytical performance; too little causes a decrease in the attraction to Ag^+ whereas too much SQD negatively affects the overall electrochemical performance of the electrode. Magnetic NPs are also suitable for Ag^+ detection [166,167]. Functionalized magnetic NPs with high affinity for Ag^+ were added to the sample and left to incubate for several minutes such that Ag^+ was adsorbed onto the NP surface. Afterwards, the NPs with adsorbed Ag^+ were brought into contact with the electrode surface by means of a magnetic electrode, and a negative potential was applied to reduce Ag^+ to metallic silver, before being re-oxidized during the stripping step. Depending on the type of NP selected, this method provides LODs between 0.13 nM and 59 nM. However, the need for addition of reagents (magnetic NPs) in the sample to be analyzed represents an evident drawback for on-site determinations.

The high affinity of silver towards several biomolecules has also encouraged the development of biosensors for the voltammetric determination of Ag^+. In particular, the interaction of silver with different nucleobases in the nucleic acids DNA and RNA encouraged the development of sensors based on cytosine-rich [135,144,168,169] or guanine-rich [170] DNA probes. Essentially, Ag^+ interacts with cytosine, stabilizing two single DNA strands via the formation of cytosine-Ag(I)-cytosine complexes [135,144] and binds with guanine, interacting through its N_7 and C_6O groups to impede its electrocatalytic oxidation [170]. Maryam et al. reported a sensor based on a CPE modified with AuNPs, including the use of ethyl green as electroactive label and two single-strand poly-cytosine DNA that were used as probe and target, respectively [144]. The presence of Ag^+ promotes the probe-target hybridization, leading to a decrease in the ethyl green signal that was proportional to the Ag^+ concentration.

Yan et al. reported on a gold electrode modified with 16-mercaptohexadecanoic acid, achieving a hydrophobic layer that isolated the electrode from any electroactive indicator present in the solution [169]. This electrode was then incubated with cysteine-rich single-stranded DNA and multi-walled carbon nanotubes (MWCNT), which only in the presence of silver were free from DNA and could assemble on the modified electrode, mediating the electron transfer and resulting in an increased signal of the electroactive indicator (Fig. 7). These two latter DNA-based strategies have reported LODs between 0.1 and 1.3 nM. However, they involve complex experimental procedures that are unlikely to be implemented in decentralized analysis of silver. The determination of trace Ag^+ was also indirectly achieved using glucose biosensors, because silver inhibits the steady-state enzymatic glucose oxidase reaction [171,172]. These sensors seemingly reach a LOD of 5 nM, with the additional advantage of high sensitivity and certainly fast analysis time, which makes them particularly suitable for continuous monitoring. As drawbacks, note that glucose concentration might need to be adjusted for different matrixes and cleaning and regeneration of the electrode takes a rather long time (4 min).

Silver-selective membranes interrogated under accumulation/stripping voltammetry method have recently been presented by Cuartero and co-workers [24,173]. The membrane has a very reduced thickness (~200 nm) and any ion-transfer occurring at the sample-membrane interface is modulated by the oxidation state of a backside connected conducting polymer (POT) [24,173-176]. In particular, POT was electrodeposited on a GCE and further modified with a thin-film membrane containing O,O"-bis[2-(methylthio)ethyl]–tert-butylcalix[4]arene as silver ionophore. The proposed interrogation method consisted of an accumulation step (E_{app} = 0 V, t = 1440s and 300 rpm) followed by the stripping of preconcentrated Ag^+ in the membrane (linear sweep voltammetry from 0 to 1.2 V at 100 mV s^{-1}). A LRR in the range of 0.05–10 nM Ag^+ concentration was reported for membranes formulated with a reduced amount of the cation-exchanger, therefore minimizing the amount of charge in the form of ion-transfer events occurring at the sample-membrane interface [173]. The electrode was successfully applied to the detection of sub-nanomolar Ag^+ levels in different water samples, including seawater.

Despite the large number of electrodes published over the last decade for the voltammetric determination of free Ag^+, their application to decentralized analysis still remains a challenge and is rarely addressed in the literature. Most of the strategies reported up to now were only tested in water samples and, in the vast majority of the cases, the water samples were spiked to reach a detectable Ag^+ concentration depending on the analytical performance of the developed electrode. Interestingly, other samples besides environmental and drinking water that have been analyzed with voltammetric silver sensors include X-ray photographic films, commercial colloidal products, human saliva, silver sulfadiazine, tea leaves or minerals [29,135,163,164,177]. However, these samples with relatively complex matrix require pre-treatment(s) ranging from relatively simple operations (such as filtration or pH adjustment) to more intricate treatments (such as acid digestion and oven drying) that make it almost impossible to bring the analytical proposal to a more decentralized level. Additionally, decentralized detection of Ag^+ by stripping voltammetry is further hindered by the calibration method. Most of the works reported on Ag^+ quantification relies on the standard addition method to account for any matrix effect. As the reader may realize, this calibration protocol requires several additions of a Ag^+ standard solution and a separate calibration procedure for each sample, two aspects that are not suitable for decentralized analysis.

3.2. Speciation between Ag^+ and AgNPs

In the particular case of silver, the ability to distinguish the speciation between Ag^+ and AgNPs is of utmost interest, given the fact that the toxicity of AgNPs is associated with the release of Ag^+ [43]. Theoretically, determining speciation between Ag^+ and AgNPs would require either the separation of the two species Ag^+ and AgNPs, which is methodologically complex and involves time-consuming processes such as filtration, centrifugation, vacuum, centrifugal ultrafiltration, or dialysis, among many others [155], or the provision of a single analytical methodology able to adequately discriminate between the two species. And indeed, some reported voltammetric electrodes show just this capability. Deamelys et al.

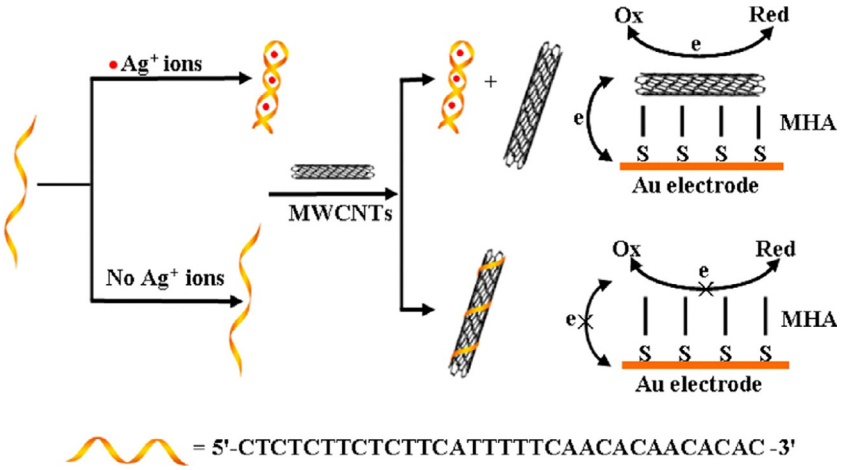

Fig. 7. Schematic illustration of the electrochemical assay for Ag^+ detection based on un-labeled C-rich ssDNA probe and controlled assembly of MWCNTs. Reproduced with permission from ref. [169].

achieved the selective determination of Ag^+ in the presence of AgNPs by ASV at a bare GCE using $NaClO_4$ as supporting electrolyte and depositing silver at –0.5 V [178]. The determination of AgNPs was achieved by calculation of the difference between Ag^+ and the total silver content, which was obtained using the same ASV protocol after acidic digestion of the sample. The results were successfully validated by atomic absorption spectrometry in combination with an ultrafiltration step that allowed for the isolation of Ag^+.

A further step was proposed by Vidal et al., who quantified both Ag^+ and AgNPs without any sample treatment [179]. The speciation of silver was performed at a GCE covalently modified with L-cysteine or electropolymerized with several oligomers (L-lysine, tiophene-3-carboxamide, thionine, and o-phenylenediamine), which allowed the accumulation of both Ag^+ and AgNPs. Two different procedures were evaluated: adsorptive stripping voltammetry (AdSV) and voltammetry of immobilized (nano)particles (ViNPs). These two procedures differ in the accumulation step; in AdSV both Ag^+ and AgNPs are accumulated at the OCP (Fig. 6b) whereas in ViNPs the sample is drop-casted onto the surface of the electrode and then dried with nitrogen. Next, the same stripping protocol is applied in both methods to achieve discrimination between Ag^+ and AgNPs. Initially, the potential is scanned toward anodic potentials (from 0.15 V to 0.45 V), which results in a voltammetric oxidation peak proportional to the amount of AgNPs present. Then, Ag^+ is determined using a reverse scan from 0.25 V to 0 V, which causes the reduction of Ag^+. Furthermore, total silver was also quantified by introducing a preelectrolysis to reduce all Ag^+ to Ag^0 prior to oxidation during the stripping step. ViNPs provided faster determinations and higher sensitivities and, in terms of electrode modification, the best analytical performance was provided by GCE electropolymerized with L –lysine, with a LOD of 93 pM and a LRR of 0.18 – 93 nM.

In terms of electrode material, AgNP determination was reported at both unmodified carbon electrodes [178] and at the so called "sticky electrodes" [180-182]. The latter offers increased capabilities toward AgNP immobilization with respect to Ag^+, which is achieved by modifying the electrode surface with molecules that contain thiol, carboxylic acid, or amine moieties, all of which present high affinity towards silver. Unmodified electrodes reached a LOD of 12 nM and a LRR of 23 – 180 nM [178] whereas "sticky electrodes" were able to measure at least 5.3 pM concentration of silver [180]. However, it is worth noting that the accumulation step reported for "sticky electrodes" is considerably longer (up to 96 h, compared to 120 s for unmodified electrodes). Spencer et al. demonstrated the selective accumulation of AgNPs in the presence of Ag^+ with a CPE modified with $Fe^{2+/3+}$ oxide NPs, achieving a LOD below 9.2 nM [183].

A common issue that has been observed in the voltammetric determination of AgNPs is that the sensitivity is strongly influenced by the size of the NP [184,185]. Thus, to obtain accurate results, calibrations must be performed with NP standards with a similar diameter to that of the target NPs [184]. This fact is a clear limitation on the potential for analysis of unknown samples, but may be overcome in the routine analysis of samples where the diameter of AgNPs diameter is well established (*e.g.* quality control of commercial products). On the other hand, when low concentrations of AgNPs are considered (< 2 mg L^{-1}) and the surface coverage of the electrode is constant and low enough to allow AgNPs to diffuse independently of each other, the peak potential will depend only on the AgNP diameter [184]. In this particular scenario, there is a linear relationship between peak potential and the Napierian logarithm of the NP diameter, which allows the use of voltammetric measurements for the characterization of AgNP size, offering a faster and cheaper alternative to more conventional techniques such as transmission electron microscopy (TEM) [186,187], dynamic light scattering (DLS) [188] or X-ray diffraction (XRD) [189].

Although AgNPs are the most common silver nanomaterial, the implementation of other silver-based nanomaterials is also gaining attention in different fields [190,191]. As novel silver nanomaterials are introduced to the market, and the differences in toxicity are assessed, determination of speciation between silver nanomaterials will also be demanded. In this context, Li et al. reported the selective determination of silver nanowires (AgNW) on an unmodified GCE [192]. The different morphologies of AgNWs and AgNPs led to a difference in the oxidation potential and the intensity of the current was used for quantification purposes, providing a LOD of 32 pM and a LRR of 46 pM – 23 nM for AgNWs.

Conclusions and future perspectives

An overview of electrochemical silver determination reported in the last decade is here presented, with an special focus on discussing the potential of potentiometric and voltammetric electrodes for decentralized analysis. Overall, the literature reflects important progress in both of these electrochemical techniques. The development of new silver ionophores, together with a better control of ion fluxes, has been demonstrated to provide enhanced analytical performance for inner-filling solution silver-selective electrodes, being suitable for trace analysis of silver in the presence of

common abundant ions. The all-solid-state format of silver potentiometric sensors is gaining more attention with a view to facilitate miniaturization as a step towards on-site measurements. Regarding the voltammetric detection of silver, bearing in mind the benefits of Ag^+ preconcentration for lowering LODs, stripping voltammetry techniques have demonstrated applicability at the subnanomolar level. Importantly, the steady rise of material science has provided novel nanomaterials that enhance the analytical performance of voltammetric sensors, and new deposition methods have also been of great value in lowering the LOD. Despite obvious advances in the direction of electrode preparation and the associated working mechanism, the potential of potentiometric and voltammetric sensors for decentralized analysis of silver has not yet been fully realized in the literature: the vast majority of the papers published in the last decade still target lab-bench applications, with only few works attempting more novel applications such as silver speciation (between Ag^+ and AgNPs). Accordingly, future efforts should be focused on assessing the real possibilities for application in decentralized silver analysis. For this purpose, evaluation of the performance of new silver selective electrodes should not focus solely on improving traditional analytical parameters (*i.e.* selectivity, sensitivity, limit of detection) but also on the assessment of crucial aspects for decentralized analysis, such as robustness, long-term stability, biofouling resistance, calibration-free methods, miniaturization, and reduced analysis times.

Credit author statement

K.X. and C.P.-R. developed the literature search and pertinent discussion and prepared the original draft. K.X. and C.P.-R. have contributed equally to this manuscript and therefore, they are sharing the first authorship. M.C. and G.A.C. conceived the paper, checked the interpretation of the selected papers, supervised, and edited the provided information and discussions. All authors took part in the visualization, writing, review, and editing the manuscript. All authors have read and agreed to the published version of the manuscript.

Declaration of Competing Interest

The authors declare that they have no known competing financial interests or personal relationships that could have appeared to influence the work reported in this paper.

Acknowledgments

G.A.C. acknowledges the KTH Royal Institute of Technology (Starting Grant, K-2017-0371), the Swedish Research Council (VR-2017-4887) and the Stiftelsen Olle Engkvist Byggmästare (194-0731). M.C. thanks the Swedish Research Council (Grant VR-2019-04142) and the ÅForsk Foundation (Grant Agreement 19-464). K.X. gratefully thanks the China Scholarship Council for supporting his Ph.D. studies.

References

[1] T.S. Institute, Silver Supply and Demand, 2020. Last accessed on: 20th Nov 2020, https://www.silverinstitute.org/silver-supply-demand/.
[2] L. Lander, R. Reuther, Metals in Society and in the Environment: A critical Review of Current Knowledge on Fluxes, Speciation, Bioavailability and Risk For Adverse Effects of Copper, Chromium, Nickel and Zinc, Kluwer Academic Publishers, New York, Boston, Dordrecht, London, Moscow, 2004.
[3] Guidelines for Drinking-Water Quality, 4th Edition, W.H. Organization, Geneva, Switzerland, 2011.
[4] H.T. Ratte, Bioaccumulation and toxicity of silver compounds: a review, Environ. Toxicol. Chem. 18 (1999) 89, doi:10.1002/etc.5620180112.
[5] T.W. Purcell, J.J. Peters, Sources of silver in the environment, Environ. Toxicol. Chem. 17 (1998) 539, doi:10.1002/etc.5620170404.
[6] S.N. Luoma, Silver Nanotechnologies and the Environment: Old Problems or New Challenges?, Woodrow Wilson International Center for Scholars, Washington DC, 2008.
[7] E. McGillicuddy, I. Murray, S. Kavanagh, L. Morrison, A. Fogarty, M. Cormican, P. Dockery, M. Prendergast, N. Rowan, D. Morris, Silver nanoparticles in the environment: sources, detection and ecotoxicology, Sci. Total Environ. 575 (2017) 231, doi:10.1016/j.scitotenv.2016.10.041.
[8] R. de Lima, A.B. Seabra, N. Duran, Silver nanoparticles: a brief review of cytotoxicity and genotoxicity of chemically and biogenically synthesized nanoparticles, J. Appl. Toxicol. 32 (2012) 867, doi:10.1002/jat.2780.
[9] F. Valverde, M. Costas, F. Pena, I. Lavilla, C. Bendicho, Determination of total silver and silver species in coastal seawater by inductively-coupled plasma mass spectrometry after batch sorption experiments with Chelex-100 resin, Chem. Speciat. Bioavailab. 20 (2015) 217, doi:10.3184/095422908x381306.
[10] D.M. Mitrano, A. Barber, A. Bednar, P. Westerhoff, C.P. Higgins, J.F. Ranville, Silver nanoparticle characterization using single particle ICP-MS (SP-ICP-MS) and asymmetrical flow field flow fractionation ICP-MS (AF4-ICP-MS), J. Anal. At. Spectrom 27 (2012) 1131, doi:10.1039/c2ja30021d.
[11] X. Wang, H. Yang, K. Li, Y. Xiang, Y. Sha, M. Zhang, X. Yuan, K. Huang, Recent developments of the speciation analysis methods for silver nanoparticles and silver ions based on atomic spectrometry, Appl. Spectrosc. Rev. 55 (2019) 509, doi:10.1080/05704928.2019.1684303.
[12] C. Gasbarri, F. Ruggieri, M. Foschi, A. Aceto, L. Scotti, G. Angelini, Simple determination of silver nanoparticles concentration as Ag^+ by using ISE as potential alternative to ICP optical emission spectrometry, Chem. Select 4 (2019) 9501, doi:10.1002/slct.201902336.
[13] P. Anekthirakun, A. Imyim, Separation of silver ions and silver nanoparticles by silica based-solid phase extraction prior to ICP-OES determination, Microchem. J. 145 (2019) 470, doi:10.1016/j.microc.2018.11.008.
[14] N. Akaighe, R.I. Maccuspie, D.A. Navarro, D.S. Aga, S. Banerjee, M. Sohn, V.K. Sharma, Humic acid-induced silver nanoparticle formation under environmentally relevant conditions, Environ. Sci. Technol. 45 (2011) 3895, doi:10.1021/es103946g.
[15] N.F. Adegboyega, V.K. Sharma, K. Siskova, R. Zboril, M. Sohn, B.J. Schultz, S. Banerjee, Interactions of aqueous Ag^+ with fulvic acids: mechanisms of silver nanoparticle formation and investigation of stability, Environ. Sci. Technol. 47 (2013) 757, doi:10.1021/es302305f.
[16] Y. Yin, J. Liu, G. Jiang, Sunlight-induced reduction of ionic Ag and Au to metallic nanoparticles by dissolved organic matter, ACS Nano 6 (2012) 7910, doi:10.1021/nn302293r.
[17] O. Długosz, M. Banach, Continuous production of silver nanoparticles and process control, J. Clust. Sci. 30 (2019) 541, doi:10.1007/s10876-019-01505-y.
[18] M. Cuartero, M. Parrilla, G.A. Crespo, Wearable potentiometric sensors for medical applications, Sensors 19 (2019) 363, doi:10.3390/s19020363.
[19] M. Cuartero, G.A. Crespo, All-solid-state potentiometric sensors: a new wave for *in situ* aquatic research, Curr. Opin. Electrochem. 10 (2018) 98, doi:10.1016/j.coelec.2018.04.004.
[20] M. Cuartero, N. Pankratova, T. Cherubini, G.A. Crespo, F. Massa, F. Confalonieri, E. Bakker, In situ detection of species relevant to the carbon cycle in seawater with submersible potentiometric probes, Environ. Sci. Technol. Lett. 4 (2017) 410, doi:10.1021/acs.estlett.7b00388.
[21] R. Athavale, C. Dinkel, B. Wehrli, E. Bakker, G.A. Crespo, A. Brand, Robust solid-contact ion selective electrodes for high-resolution *in situ* measurements in fresh water systems, Environ. Sci. Technol. Lett. 4 (2017) 286, doi:10.1021/acs.estlett.7b00130.
[22] R. Athavale, I. Kokorite, C. Dinkel, E. Bakker, B. Wehrli, G.A. Crespo, A. Brand, In situ ammonium profiling using solid-contact ion-selective electrodes in eutrophic lakes, Anal. Chem. 87 (2015) 11990, doi:10.1021/acs.analchem.5b02424.
[23] G.A. Crespo, Recent advances in ion-selective membrane electrodes for *in situ* environmental water analysis, Electrochim. Acta. 245 (2017) 1023, doi:10.1016/j.electacta.2017.05.159.
[24] K. Xu, M. Cuartero, G.A. Crespo, Lowering the limit of detection of ion-selective membranes backside contacted with a film of poly(3-octylthiophene), Sens. Actuat. B Chem. 297 (2019) 126781, doi:10.1016/j.snb.2019.126781.
[25] G. Lisak, T. Tamaki, T. Ogawa, Dualism of sensitivity and selectivity of porphyrin dimers in electroanalysis, Anal. Chem. 89 (2017) 3943, doi:10.1021/acs.analchem.6b04179.
[26] A. Afkhami, A. Shirzadmehr, T. Madrakian, H. Bagheri, New nano-composite potentiometric sensor composed of graphene nanosheets/thionine/molecular wire for nanomolar detection of silver ion in various real samples, Talanta 131 (2015) 548, doi:10.1016/j.talanta.2014.08.004.
[27] A. Dadkhah, M.K. Rofouei, M.H. Mashhadizadeh, Synthesis and characterization of N,N′-bis(benzophenone imine)formamidine as ionophores for silver-selective electrodes, Sens. Actuat. B Chem. 202 (2014) 410, doi:10.1016/j.snb.2014.05.090.
[28] Q. Liu, J. Li, W. Yang, X. Zhang, C. Zhang, C. Labbe, X. Portier, F. Liu, J. Yao, B. Liu, Simultaneous detection of trace Ag(I) and Cu(II) ions using homoepitaxially grown GaN micropillar electrode, Anal. Chim. Acta 1100 (2020) 22, doi:10.1016/j.aca.2019.11.010.
[29] S.M. Ghalebi, V. Zare-Shahabadi, H. Parham, A carbon paste electrode modified with poly(methylene disulfide) nanoparticles for anodic stripping voltammetric determination of silver(I), Microchim. Acta 186 (2019) 60, doi:10.1007/s00604-018-3156-0.

[30] H. El-Mai, E. Espada-Bellido, M. Stitou, M. Garcia-Vargas, M.D. Galindo-Riano, Determination of ultra-trace amounts of silver in water by differential pulse anodic stripping voltammetry using a new modified carbon paste electrode, Talanta 151 (2016) 14, doi:10.1016/j.talanta.2016.01.008.

[31] T.J. Davies, Anodic stripping voltammetry with graphite felt electrodes for the trace analysis of silver, Analyst 141 (2016) 4742, doi:10.1039/c6an00590j.

[32] J.L. Barriada, A.D. Tappin, E.H. Evans, E.P. Achterberg, Dissolved silver measurements in seawater, Trends Anal. Chem. 26 (2007) 809, doi:10.1016/j.trac.2007.06.004.

[33] A.M. Dietrich, EPA Secondary Maximum Contaminant Levels: A strategy For Drinking Water Quality and Consumer Acceptability. U.S.A., 2015.

[34] G. Scoccianti, F. Frenos, G. Beltrami, D.A. Campanacci, R. Capanna, Levels of silver ions in body fluids and clinical results in silver-coated megaprostheses after tumour, trauma or failed arthroplasty, Injury 47 (2016) S11, doi:10.1016/j.injury.2016.07.042.

[35] N. Wasukan, S. Srisung, K. Kulthong, S. Boonrungsiman, R. Maniratanachote, Determination of silver in personal care nanoproducts and effects on dermal exposure, J. Nanopart. Res. 17 (2015) 425, doi:10.1007/s11051-015-3220-1.

[36] J.E. Reddy, Groundwater Quality in the Genesee river Basin, US Geological Survey, New York, 2010.

[37] T.G.Kazi Naeemullah, H.I. Afridi, F. Shah, S.S. Arain, K.D. Brahman, J. Ali, M.S. Arain, Simultaneous determination of silver and other heavy metals in aquatic environment receiving wastewater from industrial area, applying an enrichment method, Arab. J. Chem. 9 (2016) 105, doi:10.1016/j.arabjc.2014.10.027.

[38] L. Li, G. Hartmann, M. Döblinger, M. Schuster, Quantification of nanoscale silver particles removal and release from municipal wastewater treatment plants in Germany, Environ. Sci. Technol. 47 (2013) 7317, doi:10.1021/es3041658.

[39] L.C. Savery, Global assessment of silver pollution using sperm whales (physeter macrocephalus) as an indicator species, J. Environ. Anal. Toxicol. 03 (2013) 1000169, doi:10.4172/2161-0525.1000169.

[40] R. Kaegi, B. Sinnet, S. Zuleeg, H. Hagendorfer, E. Mueller, R. Vonbank, M. Boller, M. Burkhardt, Release of silver nanoparticles from outdoor facades, Environ. Pollut. 158 (2010) 2900, doi:10.1016/j.envpol.2010.06.009.

[41] A. Massarsky, V.L. Trudeau, T.W. Moon, Predicting the environmental impact of nanosilver, Environ. Toxicol. Pharmacol. 38 (2014) 861, doi:10.1016/j.etap.2014.10.006.

[42] A. Singh, W.C. Hou, T.F. Lin, R.G. Zepp, Roles of silver-chloride complexations in sunlight-driven formation of silver nanoparticles, Environ. Sci. Technol. 53 (2019) 11162, doi:10.1021/acs.est.9b02115.

[43] X. Yang, A.P. Gondikas, S.M. Marinakos, M. Auffan, J. Liu, H. Hsu-Kim, J.N. Meyer, Mechanism of silver nanoparticle toxicity is dependent on dissolved silver and surface coating in Caenorhabditis elegans, Environ. Sci. Technol. 46 (2012) 1119, doi:10.1021/es202417t.

[44] K.Y. Chumbimuni-Torres, Z. Dai, N. Rubinova, Y. Xiang, E. Pretsch, J. Wang, E. Bakker, Potentiometric biosensing of proteins with ultrasensitive ion-selective microelectrodes and nanoparticle labels, J. Am. Chem. Soc. 128 (2007) 13676, doi:10.1021/ja065899k.

[45] A.L. Gallo, F. Paladini, A. Romano, T. Verri, A. Quattrini, A. Sannino, M. Pollini, Efficacy of silver coated surgical sutures on bacterial contamination, cellular response and wound healing, Mater. Sci. Eng. C. 69 (2016) 884, doi:10.1016/j.msec.2016.07.074.

[46] H. Zhang, V. Oyanedel-Craver, Evaluation of the disinfectant performance of silver nanoparticles in different water chemistry conditions, J. Environ. Eng. 138 (2012) 58, doi:10.1061/(ASCE)EE.1943-7870.0000460.

[47] T.-M. Hseu, G.A. Rechnitz, Analytical study of a sulfide ion-selective membrane electrode in alkaline solution, Anal. Chem. 40 (1968) 1054, doi:10.1021/ac60263a020.

[48] R. De Marco, R. Cattrall, J.Liesegang W., G.L. Nyberg, Surface studies of the silver sulfide ion selective electrode membrane, Anal. Chem. 62 (1990) 2339, doi:10.1021/ac00220a015.

[49] M.-T. Lai, J.-S. Shih, Mercury(II) and silver(I) ion-selective electrodes based crown ethers, Analyst 111 (1986) 891, doi:10.1039/AN9861100891.

[50] J. Bobacka, T. Lahtinen, J. Nordman, S. Häggström, K. Rissanen, A. Lewenstam, A. Ivaska, All-solid-state Ag+ - ISE based on [2.2.2]p,p,p-cyclophane, Electroanalysis 13 (2001) 723. doi:10.1002/1521-4109(200105)13:8/9<723::AID-ELAN723>3.0.CO;2-R.

[51] A. Cadogan, Z. Gao, A. Lewenstam, A. Ivaska, D. Diamond All-solid-state sodium-selective electrode based on a calixarene ionophore in a poly (vinyl chloride) membrane with a polypyrrole solid contact, Ana. Chem. 64 (1992) 2496, doi:10.1021/ac00045a007.

[52] G.H. Rounaghi, A. Ghaemi, A Silver(I) selective PVC membrane electrode based on 1,13-Bis(8-quinolyl)-1,4,7,10,13-pentaoxatridecane as an ionophore, J. Electrochem. Soc. 159 (2012) F97, doi:10.1149/2.113204jes.

[53] Z. Yan, Y. Lu, H. Wang, S. Wu, B. Zhao, A heterocycle functionalized p-tert-butylcalix[4]arene as a neutral carrier for silver(I) ion-selective electrode, J. Mol. Liq. 183 (2013) 72, doi:10.1016/j.molliq.2013.04.011.

[54] W. Janrungroatsakul, C. Lertvachirapaiboon, W. Ngeontae, W. Aeungmaitrepirom, O. Chailapakul, S. Ekgasit, T. Tuntulani, Development of coated-wire silver ion selective electrodes on paper using conductive films of silver nanoparticles, Analyst 138 (2013) 6786, doi:10.1039/c3an01385e.

[55] J. Zhang, S.Y. Yu, T.J. Yin, X.F. Hu, W. Qin, A comparative study of four 20-membered N_2S_4-crown ethers as ionophores for polymeric membrane silver selective electrodes, Chin. Chem. Lett. 21 (2010) 464, doi:10.1016/j.cclet.2009.11.028.

[56] M. Shamsipur, B. Hashemi, S. Dehdashtian, M. Mohammadi, M.B. Gholivand, A. Garau, V. Lippolis, Silver ion imprinted polymer nanobeads based on a azathioether crown containing a 1,10-phenanthroline subunit for solid phase extraction and for voltammetric and potentiometric silver sensors, Anal. Chim. Acta 852 (2014) 223, doi:10.1016/j.aca.2014.09.028.

[57] N.R. Gupta, S.K.A. Kumar, S.K. Mittal, P. Singh, S. Kumar, Silver selective electrodes using ionophores functionalized with thioether–amide–amine, J. Anal. Chem. 72 (2017) 191, doi:10.1134/s1061934817020083.

[58] M.A. Arada Pérez, L.L. Duharte, M. Yazdani-Pedram, Study and characterization of a silver-selective membrane electrode based on 5-(4-dimethylaminobenzylidene)rhodanine, Port, Electrochim. Acta 37 (2019) 373, doi:10.4152/pea.201906373.

[59] O.A. Omran, F.A. Elgendy, A. Nafady, Fabrication and applications of potentiometric sensors based on p-tert-butylthiacalix[4]arene comprising two triazole rings ionophore for silver ion detection, Int. J. Electrochem. Sci. 11 (2016) 4729, doi:10.20964/2016.06.35.

[60] M.E.M. Hassouna, S.A.A. Elsuccary, J.P. Graham, N,N′-Bis(3-methyl-1-phenyl-4-benzylidine-5-pyrazolone)propylenediamine Schiff base as a neutral carrier for silver(I) ion-selective electrodes, Sens. Actuat. B Chem. 146 (2010) 79, doi:10.1016/j.snb.2010.02.012.

[61] E. Jeong, M.S. Ahmed, H.-S. Jeong, E.-H. Lee, S.-W. Jeon, Novel silver(I) ion selective PVC membrane electrode based on the schiff base ($N^2E,N^{2'}E$)-$N^2,N^{2'}$-bis(thiophen-2-ylmethylene)-1,1′-binaphthyl-2,2′-diamine, B. Korean Chem. Soc. 32 (2011) 800, doi:10.5012/bkcs.2011.32.3.800.

[62] C.-Z. Lai, M.A. Fierke, R. Correa da Costa, J.A. Gladysz, A. Stein, P. Bühlmann, Highly selective detection of silver in the low ppt range with ion-selective electrodes based on ionophore-doped fluorous membranes, Anal. Chem. 82 (2010) 7634, doi:10.1021/ac1013767.

[63] E. Malinowska, Z. Brzózka, K. Kasiura, R.J. Egberink, D.N. Reinhoudt, Silver selective electrodes based on thioether functionalized calix [4]arenes as ionophores, Anal. Chim Acta 298 (1994) 245.

[64] R. Ludwig, Calixarenes in analytical and separation chemistry, Fresenius' J. of Anal. Chem. 367 (2000) 103.

[65] V.K. Gupta, M.K. Pal, A.K. Singh, Comparative study of Ag(I) selective poly(vinyl chloride) membrane sensors based on newly developed Schiff-base lariat ethers derived from 4,13-diaza-18-crown-6, Anal. Chim. Acta 631 (2009) 161, doi:10.1016/j.aca.2008.10.033.

[66] H. Brown, J. Terrence, P. Vasquez, D.W. Bates, E. Zimlichman, Continuous monitoring in an inpatient medical-surgical unit: a controlled clinical trial, Am. J. Med. Sci. 127 (2014) 226, doi:10.1016/j.amjmed.2013.12.004.

[67] C. Yu, S. Qian, X. Qin, J. Zhang, The synthesis of thiaazacrown ethers containing pyridine as subuint for the construction of Ag^+-ISEs, Int. J. Electrochem. Sci. 8 (2013) 8544.

[68] M.H. Mashhadizadeh, R.P. Talemi, A. Shockravi, M. Kamali, Comparative studies on carbon paste electrodes based on three dithiocarbamate podands as ionophore in Ag(I) sensors, Anal. Methods 4 (2012) 742, doi:10.1039/c2ay05559g.

[69] M.H. Mashhadizadeh, A. Shockravi, Z. Khoubi, D. Heidarian, Efficient synthesis of a new podand and application as a suitable carrier for silver ion-selective electrode, Electroanalysis 21 (2009) 1041, doi:10.1002/elan.200804513.

[70] M.M. Ardakani, H. Dehghani, M. Jalayer, H.R. Zare, Potentiometric determination of silver(I) by selective membrane electrode based on derivative of porphyrin, Analyt. Sci. 20 (2004) 1667, doi:10.2116/analsci.20.1667.

[71] J.H. On, K.T. Cho, Y. Park, S. Hahm, W. Kim, J.Y. Cho, J.H. Hwang, Y.M. Jun, G.S. Cha, H. Nam, B.H. Kim, Synthesis of 7-deoxycholic amides or cholanes containing distinctive ion-recognizing groups at C3 and C12 and evaluation for ion-selective ionophores, Tetrahedron 65 (2009) 1415, doi:10.1016/j.tet.2008.12.023.

[72] F. Mizani, A. Shockravi, M. Taghdiri, S. Bavili Tabrizi, F. Azmoodeh, K. Alizadeh, M. Shamsipur, Synthesis, metal ion complexation and first use of a thia-aza substituted macrocyclic diamide as a novel sensing material for preparation of selective and sensitive poly(vinyl chloride)-membrane potentiometric sensors for Ag+ ion, J. Incl. Phenom. Macrocycl. Chem. 79 (2014) 83, doi:10.1007/s10847-013-0327-9.

[73] A.K. Singh, P. Saxena, Silver(I)-selective electrode based on [Bz_2Oxo_4(18)dieneS_4] tetrathia macrocyclic carrier, Anal. Bioanal. Chem. 385 (2006) 90, doi:10.1007/s00216-006-0385-6.

[74] A. Kumar, B. Patel, G. Patel, S.K. Menon, Potentiometric biosensing of glucose by fullerene-based silver selective electrodes, Fuller. Nanotub. Carbon Nanostructures 18 (2010) 186, doi:10.1080/15363831003782890.

[75] G. Jagerszki, A. Grun, I. Bitter, K. Toth, R.E. Gyurcsanyi, Ionophore-gold nanoparticle conjugates for Ag(+)-selective sensors with nanomolar detection limit, Chem Commun 46 (2010) 607, doi:10.1039/b914430g.

[76] Z. Szigeti, A. Malon, T. Vigassy, V. Csokai, A. Grun, K. Wygladacz, N. Ye, C. Xu, V.J. Chebny, I. Bitter, R. Rathore, E. Bakker, E. Pretsch, Novel potentiometric and optical silver ion-selective sensors with subnanomolar detection limits, Anal. Chim. Acta 572 (2006) 1, doi:10.1016/j.aca.2006.05.009.

[77] W. Janrungroatsakul, T. Vilaivan, C. Vilaivan, S. Watchasit, C. Suksai, W. Ngeontae, W. Aeungmaitrepirom, T. Tuntulani, New calix[4]arene derivatives as ionophores in polymeric membrane electrodes for Ag(I): comparative selectivity studies and detection of DNA hybridization, Talanta 105 (2013) 1, doi:10.1016/j.talanta.2012.11.046.

[78] M. Shamsipur, M. Javanbakht, V. Lippolis, A. Garau, G. De Filippo, M.R. Ganjali, A. Yari, Novel Ag+ ion-selective electrodes based on two new mixed aza-

thioether crowns containing a 1,10-phenanthroline sub-unit, Anal. Chim. Acta 462 (2002) 225, doi:10.1016/S0003-2670(02)00374-4.
[79] R.M. Izatt, J.S. Bradshaw, S.A. Nielsen, J.D. Lamb, J.J. Christensen, D. Sen, Thermodynamic and kinetic data for cation-macrocycle interaction, Chem. Rev. 85 (1985) 271, doi:10.1021/cr00068a003.
[80] J. Zhang, J. Ding, T. Yin, X. Hu, S. Yu, W. Qin, Synthesis and characterization of monoazathiacrown ethers as ionophores for polymeric membrane silver-selective electrodes, Talanta 81 (2010) 1056, doi:10.1016/j.talanta.2010.01.060.
[81] J.H. Shim, I.S. Jeong, M.H. Lee, H.P. Hong, J.H. On, K.S. Kim, H.S. Kim, B.H. Kim, G.S. Cha, H. Nam, Ion-selective electrodes based on molecular tweezer-type neutral carriers, Talanta 63 (2004) 61, doi:10.1016/j.talanta.2003.12.050.
[82] B.H. Kim, H.P. Hong, K.T. Cho, J.H. On, Y.M. Jun, I.S. Jeong, G.S. Cha, H. Nam, Silver(I) ion selective ionophores containing dithiocarbamoyl moieties on steroid backbone, Talanta 66 (2005) 794, doi:10.1016/j.talanta.2004.12.033.
[83] N.K. Joon, J.E. Barnsley, R. Ding, S. Lee, R.-.M. Latonen, J. Bobacka, K.C. Gordon, T. Ogawa, G. Lisak, Silver(I)-selective electrodes based on rare earth element double-decker porphyrins, Sens. Actuat. B Chem. 305 (2020) 127311, doi:10.1016/j.snb.2019.127311.
[84] G. Jagerszki, A. Takacs, I. Bitter, R.E. Gyurcsanyi, Solid-state ion channels for potentiometric sensing, Angew. Chem. Int. Ed. Engl. 50 (2011) 1656, doi:10.1002/anie.201003849.
[85] J.L. Carey, A. Hirao, K. Sugiyama, P. Bühlmann, Semifluorinated polymers as ion-selective electrode membrane matrixes, Electroanalysis 29 (2017) 739, doi:10.1002/elan.201600586.
[86] C.S. Lee, M.E. Lutcavage, E. Chandler, D.J. Madigan, R.M. Cerrato, N.S. Fisher, Declining mercury concentrations in bluefin tuna reflect reduced emissions to the north Atlantic ocean, Environ. Sci. Technol. 50 (2016) 12825, doi:10.1021/acs.est.6b04328.
[87] F.A. Cross, D.W. Evans, R.T. Barber, Decadal declines of mercury in adult bluefish (1972-2011) from the mid-Atlantic coast of the U.S.A, Environ. Sci. Technol. 49 (2015) 9064, doi:10.1021/acs.est.5b01953.
[88] Sodium in drinking-water, World Health Organization. 2003.
[89] Drinking water advisoryConsumer Acceptability Advice and Health Effects Analysis on Sodium, U.S. Environmental Protection Agency (EPA). U.S.A, 2003.
[90] A. Ceresa, A. Radu, S. Peper, E. Bakker, E. Pretsch, Rational design of potentiometric trace level ion sensors. A Ag^+-selective electrode with a 100 ppt detection limit, Anal. Chem. 74 (2002) 4027, doi:10.1021/ac025548y.
[91] E. Bakker, Potentiometry at trace levels, Trends Anal. Chem. 20 (2001) 11, doi:10.1016/S0167-2940(01)90073-1.
[92] A. Shvarev, E. Bakker, Pulsed galvanostatic control of ionophore-based polymeric ion sensors, Anal. Chem. 75 (2003) 4541, doi:10.1021/ac034409t.
[93] T. Vigassy, R.E. Gyurcsányi, E. Pretsch, Influence of incorporated lipophilic particles on ion fluxes through polymeric ion-selective membranes, Electroanalysis 15 (2003) 375, doi:10.1002/elan.200390043.
[94] A. Ceresa, T. Sokalski, E. Pretsch, Influence of key parameters on the lower detection limit and response function of solvent polymeric membrane ion-selective electrodes, J. Electroanal. Chem. 501 (2001) 70, doi:10.1016/S0022-0728(00)00488-5.
[95] E. Bakker, Determination of unbiased selectivity coefficients of neutral carrier-based cation-selective electrodes, Anal. Chem. 69 (1997) 1061, doi:10.1021/ac960891m.
[96] S. Makarychev-Mikhailov, A. Shvarev, E. Bakker, Pulstrodes: triple pulse control of potentiometric sensors, J. Am. Chem. Soc. 126 (2004) 10548, doi:10.1021/ja047728q.
[97] K.L. Gemene, A. Shvarev, E. Bakker, Selectivity enhancement of anion-responsive electrodes by pulsed chronopotentiometry, Anal. Chim. Acta 583 (2007) 190, doi:10.1016/j.aca.2006.09.042.
[98] G.A. Crespo, E. Bakker, Dynamic electrochemistry with ionophore based ion-selective membranes, RSC Adv. 3 (2013) 25461, doi:10.1039/c3ra43751e.
[99] H. Perera, A. Shvarev, Unbiased selectivity coefficients obtained for the pulsed chronopotentiometric polymeric membrane ion sensors, J. Am. Chem. Soc. 129 (2007) 15754, doi:10.1021/ja076821m.
[100] E. Lindner, R.E. Gyurcsányi, Quality control criteria for solid-contact, solvent polymeric membrane ion-selective electrodes, J. Solid State Electrochem. 13 (2008) 51, doi:10.1007/s10008-008-0608-1.
[101] M. Parrilla, M. Cuartero, G.A. Crespo, Wearable potentiometric ion sensors, Trends Anal. Chem. 110 (2019) 303, doi:10.1016/j.trac.2018.11.024.
[102] M.H. Mashhadizadeh, A. Mostafavi, H. Allah-Abadi, I. Sheikhshoai, New Schiff base modified carbon paste and coated wire PVC membrane electrode for silver ion, Sens. Actuators B Chem. 113 (2006) 930, doi:10.1016/j.snb.2005.04.017.
[103] S.K.A. Kumar, S.K. Mittal, S. Kumar, Highly selective potentiometric determination of Ag(I) using 1,2,4,5-tetrakis(8-hydroxyquinolinoxymethyl)benzene based coated-wire ion-selective electrode, Sens. Lett. 9 (2011) 1390, doi:10.1166/sl.2011.1696.
[104] S.K. Ashok Kumar, Manjusha Shipra, Dual behavior of thiuram sulphide: highly selective transport and ion-selective electrode for Ag(I) ions under two different conditions, J. Membr. Sci. 350 (2010) 161, doi:10.1016/j.memsci.2009.12.024.
[105] J.-.P. Veder, R. De Marco, G. Clarke, R. Chester, A. Nelson, K. Prince, E. Pretsch, E. Bakker, Elimination of undesirable water layers in solid-contact polymeric ion-selective electrodes, Anal. Chem. 80 (2008) 6731, doi:10.1021/ac800823f.
[106] T. Yin, Y. Liu, W. Qin, Single-piece solid-contact polymeric membrane ion-selective electrodes for silver ion, J. Electrochem. Soc. 160 (2013) B91, doi:10.1149/2.004308jes.
[107] E. Woźnica, M.M. Wójcik, M. Wojciechowski, J. Mieczkowski, E. Bulska, K. Maksymiuk, A. Michalska, Improving the upper detection limit of potentiometric sensors, Electroanalysis 27 (2015) 720, doi:10.1002/elan.201400567.
[108] F. Hashemi, A.R. Zanganeh, Electrochemically induced regioregularity of the binding sites of a polyaniline membrane as a powerful approach to produce selective recognition sites for silver ion, J. Electroanal. Chem. 767 (2016) 24, doi:10.1016/j.jelechem.2016.02.008.
[109] G.H. Rounaghi, I. Razavipanah, M.H. Vakili-Zarch, M. Ghanei-Motlagh, M.R. Salavati, Electrochemical synthesis of Alizarin Red S doped polypyrrole and its applications in designing a novel silver(I) potentiometric and voltammetric sensor, J. Mol. Liq. 211 (2015) 210, doi:10.1016/j.molliq.2015.06.066.
[110] Ö. Isildak, N. Delİgönül, O. Özbek, A novel silver(I)-selective PVC membrane sensor and its potentiometricapplications, Turk. J. Chem. 43 (2019) 1149, doi:10.3906/kim-1812-29.
[111] N. Sohrabi-Gilani, M.H. Nasirtabrizi, A.P. Jadid, A new multiwalled carbon nanotube/copolymer based Ag (I) carbon paste electrode for potentiometric measurements, Measurement 125 (2018) 84, doi:10.1016/j.measurement.2018.04.050.
[112] S. Ramezani, M.H. Mashhadizadeh, M. Ghobadi, S. Jalilian, Silica gel/gold nanoparticles/$(NS)_2$ ligand nanoporous platform-modified ionic liquid carbon paste electrode for potentiometric ultratrace assessment of Ag(I), Int. J. Environ. Sci. Technol. 13 (2016) 2175, doi:10.1007/s13762-016-1028-x.
[113] C. Yang, Y. Chai, R. Yuan, W. Xu, T. Zhang, F. Jia, Conjugates of graphene oxide covalently linked ligands and gold nanoparticles to construct silver ion graphene paste electrode, Talanta 97 (2012) 406, doi:10.1016/j.talanta.2012.04.053.
[114] Q. Zhao, Y. Chai, R. Yuan, T. Zhang, C. Yang, A new silver(I)-selective electrode based on derivatized MWCNTs@SiO_2 nanocomposites as a neutral carrier, Mater. Sci. Eng. C. 32 (2012) 1352, doi:10.1016/j.msec.2012.04.006.
[115] T. Zhang, Y. Chai, R. Yuan, J. Guo, Nanostructured multi-walled carbon nanotubes derivate based on carbon paste electrode for potentiometric detection of Ag^+ ions, Anal. Methods 4 (2012) 454, doi:10.1039/c2ay05668b.
[116] M.H. Mashhadizadeh, S. Ramezani, A. Shockravi, M. Kamali, Comparative study of carbon paste electrodes modified by new pentaaza macrocyclic ligands and gold nanoparticles embedded in three-dimensional sol–gel network for determination of trace amounts of Ag(I), J. Incl. Phenom. Macrocycl. Chem. 76 (2013) 283, doi:10.1007/s10847-012-0197-6.
[117] T. Yin, T. Han, C. Li, W. Qin, J. Bobacka, Real-time monitoring of the dissolution of silver nanoparticles by using a solid-contact Ag(+)-selective electrode, Anal. Chim. Acta 1101 (2020) 50, doi:10.1016/j.aca.2019.12.022.
[118] H.M. Abu-Shawish, S.M. Saadeh, H.M. Dalloul, B. Najri, H.A. Athamna, Modified carbon paste electrode for potentiometric determination of silver(I) ions in burning cream and radiological films, Sens. Actuat. B Chem. 182 (2013) 374, doi:10.1016/j.snb.2013.03.018.
[119] W. Ngeontae, W. Janrungroatsakul, P. Maneewattanapinyo, S. Ekgasit, W. Aeungmaitrepirom, T. Tuntulani, Novel potentiometric approach in glucose biosensor using silver nanoparticles as redox marker, Sens. Actuat. B Chem. 137 (2009) 320, doi:10.1016/j.snb.2008.11.003.
[120] W. Ngeontae, W. Janrungroatsakul, N. Morakot, W. Aeungmaitrepirom, T. Tuntulani, New silver selective electrode fabricated from benzothiazole calix[4]arene: speciation analysis of silver nanoparticles, Sens. Actuat. B Chem. 134 (2008) 377, doi:10.1016/j.snb.2008.05.010.
[121] J.B. Czirok, G. Jágerszki, K. Tóth, Á. Révész, L. Drahos, I. Bitter, Click synthesis of triazole-linked calix[4]arene ionophores. Potentiometric and ESI-MS screening of ion-selectivity, J. Incl. Phenom. Macro. Chem. 78 (2013) 207, doi:10.1007/s10847-013-0289-y.
[122] E. Lee, E. Jeong, S. Jeon, A potentiometric sensor of silver ions based on the Schiff base of diphenol, J. Solid State Electrochem. 16 (2012) 2591, doi:10.1007/s10008-012-1682-y.
[123] H.-.R. Seo, E.-.S. Jeong, M.S. Ahmed, H.-.K. Lee, S.-.W. Jeon, Polymeric membrane silver-ion selective electrodes based on schiff base N,N'-bis(pyridin-2-ylmethylene)benzene-1,2-diamine, B. Korean Chem. Soc. 31 (2010) 1699, doi:10.5012/bkcs.2010.31.6.1699.
[124] M. Mohammadi, M. Khodadadian, M.K. Rofouei, A. Beiza, A.R. Jalalvand, Monitoring trace amounts of silver(I) in water samples using a potentiometric sensor based on 1,3-bis(2-ethoxyphenyl)triazene, Sens. Lett. 8 (2010) 285, doi:10.1166/sl.2010.1265.
[125] K. Mehdizadeh, M. Giahi, H. Aghaie, Design and manufacture of silver-selective electrode based on single-walled carbon nanotubes, Orient. J. Chem. 31 (2015) 703, doi:10.13005/ojc/310212.
[126] K. Mehdizadeh, M. Giahi, H. Aghaie, Single-walled carbon nanotubes functionalized with N-(6-aminohexyl) carboxamide as ionophore for sensing silver ions, J. Anal. Chem. 73 (2018) 383, doi:10.1134/s1061934818040093.
[127] Q. Zhao, Y. Chai, R. Yuan, T. Zhang, Z. Zou, A new silver ion-selective electrodes based on derivatized multi-walled carbon nanotubes as neutral carriers, Sens. Lett. 10 (2012) 96, doi:10.1166/sl.2012.2317.
[128] T. Zhang, Y. Chai, R. Yuan, J. Guo, Potentiometric detection of silver(I) ion based on carbon paste electrode modified with diazo-thiophenol-functionalized nanoporous silica gel, Mater. Sci. Eng. C. 32 (2012) 1179, doi:10.1016/j.msec.2012.03.005.
[129] D.M. Sejmanović, B.B. Petković, M.V. Budimir, S.P. Sovilj, V.M. Jovanović, Characterization of a silver modified PVCAc electrode and its application as a Ag(I)-Selective potentiometric sensor, Electroanalysis 23 (2011) 1849, doi:10.1002/elan.201000745.
[130] S. Singh, G. Rani, M. Zhu, Silver selective electrode based on hybrid meso-

porous silica (MCM-41) modified material, Electroanalysis 31 (2019) 1562, doi:10.1002/elan.201900050.
[131] T. Alizadeh, F. Rafiei, An innovative application of graphitic carbon nitride (g-C_3N_4) nano-sheets as silver ion carrier in a solid state potentiometric sensor, Mater. Chem. Phys. 227 (2019) 176, doi:10.1016/j.matchemphys.2019.01.060.
[132] M.R. Zhang, G.B. Pan, Porous GaN electrode for anodic stripping voltammetry of silver(I), Talanta 165 (2017) 540, doi:10.1016/j.talanta.2017.01.016.
[133] F. Wang, C. Xin, Y. Wu, Y. Gao, B. Ye, Anodic stripping voltammetric determination of silver(I) in water using a 4-tert-butyl-1(ethoxycarbonylmethoxy)thiacalix[4]arene modified glassy carbon electrode, J. Anal. Chem. 66 (2011) 60, doi:10.1134/s1061934811010047.
[134] M.C. Radulescu, A. Chira, M. Radulescu, B. Bucur, M.P. Bucur, G.L. Radu, Determination of silver(I) by differential pulse voltammetry using a glassy carbon electrode modified with synthesized N-(2-aminoethyl)-4,4′-bipyridine, Sensors 10 (2010) 11340, doi:10.3390/s101211340.
[135] Y. Wu, R.Y. Lai, A reagentless DNA-based electrochemical silver(I) sensor for real time detection of Ag(I) - the effect of probe sequence and orientation on sensor response, Biotechnol. J. 11 (2016) 788, doi:10.1002/biot.201500428.
[136] L. Fu, A. Wang, K. Xie, J. Zhu, F. Chen, H. Wang, H. Zhang, W. Su, Z. Wang, C. Zhou, S. Ruan, Electrochemical detection of silver ions by using sulfur quantum dots modified gold electrode, Sens. Actuat. B Chem. 304 (2020) 127390, doi:10.1016/j.snb.2019.127390.
[137] M.B. Gholivand, M.H. Parvin, Differential pulse anodic stripping voltammetric simultaneous determination of copper(II) and silver(I) with bis(2-hydroxyacetophenone) butane-2,3-dihydrazone modified carbon paste electrodes, Electroanalysis 22 (2010) 2291, doi:10.1002/elan.201000190.
[138] M.A. Gulppi, N. Vejar, L. Tamayo, M.I. Azocar, C. Vera, C. Silva, J.H. Zagal, F. Scholz, M.A. Páez, Stripping voltammetry microprobe (SPV): a new approach in electroanalysis, Electrochem. Commun. 41 (2014) 8, doi:10.1016/j.elecom.2014.01.012.
[139] M. Gulppi, J. Pavez, J.H. Zagal, M. Sancy, M. Azocar, F. Scholz, M.A. Páez, Stripping voltammetry microprobe (SPV): substantial improvements of the protocol, J. Electroanal. Chem. 745 (2015) 61, doi:10.1016/j.jelechem.2015.03.008.
[140] Y.H. Li, H.Q. Xie, F.Q. Zhou, Alizarin violet modified carbon paste electrode for the determination of trace silver(I) by adsorptive voltammetry, Talanta 67 (2005) 28, doi:10.1016/j.talanta.2005.02.009.
[141] K.S. Ha, J.H. Kim, Y.S. Ha, S.S. Lee, M.L. Seo, Anodic stripping voltammetric determination of silver(I) at a carbon paste electrode modified with S2o2-donor podand, Anal. Lett. 34 (2007) 675, doi:10.1081/al-100103211.
[142] H. Gellon, P.S. González, C.A. Fontan, Square wave anodic stripping determination of silver using a carbon paste electrode modified with a strong acid ion-exchanger, Anal. Lett. 36 (2003) 2749, doi:10.1081/al-120025253.
[143] S. Tanaka, H. Yoshida, Stripping voltammetry of silver (I) with a carbon-paste electrode modified with thiacrown compounds, Talanta 36 (1989) 1044, doi:10.1016/0039-9140(89)80191-2.
[144] M. Ebrahimi, J.B. Raoof, R. Ojani, Novel electrochemical DNA hybridization biosensors for selective determination of silver ions, Talanta 144 (2015) 619, doi:10.1016/j.talanta.2015.07.020.
[145] S. Jahandari, M.A. Taher, H. Fazelirad, I. Sheikhshoai, Anodic stripping voltammetry of silver(I) using a carbon paste electrode modified with multi-walled carbon nanotubes, Microchim. Acta 180 (2013) 347, doi:10.1007/s00604-012-0935-x.
[146] Z. Bi, P. Salaun, C.M. van den Berg, Determination of lead and cadmium in seawater using a vibrating silver amalgam microwire electrode, Anal. Chim. Acta 769 (2013) 56, doi:10.1016/j.aca.2013.01.049.
[147] I.G. Švegl, M. Kolar, B. Ogorevc, B. Pihlar, Vermiculite clay mineral as an effective carbon paste electrode modifier for the preconcentration and voltammetric determination of Hg (II) and Ag (I) ions, J. Anal. Chem. 361 (1998) 358, doi:10.1007/s002160050904.
[148] C. Pérez-Ràfols, N. Serrano, J. Manuel Díaz-Cruz, C. Ariño, M. Esteban, A screen-printed voltammetric electronic tongue for the analysis of complex mixtures of metal ions, Sens. Actuat. B Chem. 250 (2017) 393, doi:10.1016/j.snb.2017.04.165.
[149] J. Barek, J. Zima, Eighty years of polarography: history and future, Electroanalysis 15 (2003) 467, doi:10.1002/elan.200390055.
[150] J. Barek, A.G. Fogg, A. Muck, J. Zima, Polarography and voltammetry at mercury electrodes, Crit. Rev. Anal. Chem. 31 (2001) 291, doi:10.1080/20014091076776.
[151] J. Hubmann, B. J., D. Monnier, Determination of trace amounts of silver(I) by polarographic. Anodic stripping and chronopotentiometric methods at a mercury electrode: studies in aqueous and nonaqueous media, Anal. Chim. Acta 62 (1972) 394, doi:10.1016/0003-2670(72)80048-5.
[152] C. Ariño, N. Serrano, J.M. Díaz-Cruz, M. Esteban, Voltammetric determination of metal ions beyond mercury electrodes. A review, Anal. Chim. Acta 990 (2017) 11, doi:10.1016/j.aca.2017.07.069.
[153] N. Serrano, J.M. Díaz-Cruz, C. Ariño, M. Esteban, Antimony- based electrodes for analytical determinations, Trends Anal. Chem. 77 (2016) 203, doi:10.1016/j.trac.2016.01.011.
[154] N. Serrano, A. Alberich, J.M. Díaz-Cruz, C. Ariño, M. Esteban, Coating methods, modifiers and applications of bismuth screen-printed electrodes, Trends Anal. Chem. 46 (2013) 15, doi:10.1016/j.trac.2013.01.012.
[155] T. Romih, S.B. Hočevar, A. Jemec, D. Drobne, Bismuth film electrode for anodic stripping voltammetric measurement of silver nanoparticle dissolution, Electrochim. Acta. 188 (2016) 393, doi:10.1016/j.electacta.2015.11.110.
[156] J. Tashkhourian, S. Javadi, F.N. Ana, Anodic stripping voltammetric determination of silver ion at a carbon paste electrode modified with carbon nanotubes, Microchim. Acta 173 (2011) 79, doi:10.1007/s00604-010-0528-5.
[157] V.Y. Maldonado, P.J. Espinoza-Montero, C.A. Rusinek, G.M. Swain, Analysis of Ag(I) biocide in water samples using anodic stripping voltammetry with a boron-doped diamond disk electrode, Anal. Chem. 90 (2018) 6477, doi:10.1021/acs.analchem.7b04983.
[158] Y. Guo, N. Huang, B. Yang, C. Wang, H. Zhuang, Q. Tian, Z. Zhai, L. Liu, X. Jiang, Hybrid diamond/graphite films as electrodes for anodic stripping voltammetry of trace Ag^+ and Cu^{2+}, Sens. Actuat. B Chem. 231 (2016) 194, doi:10.1016/j.snb.2016.02.098.
[159] Q.Y. Liu, B.D. Liu, F. Yuan, H. Zhuang, C. Wang, D. Shi, Y.K. Xu, X. Jiang, Anodic stripping voltammetry of silver(I) using unmodified GaN film and nanostructure electrodes, Appl. Surf. Sci. 356 (2015) 1058, doi:10.1016/j.apsusc.2015.08.167.
[160] H. Zhuang, C. Wang, N. Huang, X. Jiang, Cubic SiC for trace heavy metal ion analysis, Electrochem. Commun. 41 (2014) 5, doi:10.1016/j.elecom.2014.01.008.
[161] N. Yang, H. Zhuang, R. Hoffmann, W. Smirnov, J. Hees, X. Jiang, C.E. Nebel, Nanocrystalline 3C-SiC electrode for biosensing applications, Anal. Chem 83 (2011) 5827, doi:10.1021/ac201315q.
[162] P. Sidambaram, J. Colleran, Nanomole silver detection in chloride-free phosphate buffer using platinum and gold micro- and nanoelectrodes, J. Electrochem. Soc. 166 (2019) B532, doi:10.1149/2.1371906jes.
[163] T. Rohani, M.A. Taher, Preparation of a carbon ceramic electrode modified by 4-(2-pyridylazo)-resorcinol for determination of trace amounts of silver, Talanta 80 (2010) 1827, doi:10.1016/j.talanta.2009.10.029.
[164] H.H. Nadiki, M.A. Taher, H. Ashkenani, I. Sheikhshoai, Fabrication of a new multi-walled carbon nanotube paste electrode for stripping voltammetric determination of Ag(I), Analyst 137 (2012) 2431, doi:10.1039/c2an16004h.
[165] J.B. Raoof, R. Ojani, A. Alinezhad, S.Z. Rezaie, Differential pulse anodic stripping voltammetry of silver(I) using p-isopropylcalix[6]arene modified carbon paste electrode, Monatsh. Chem. - Chem. Month. 141 (2010) 279, doi:10.1007/s00706-010-0258-8.
[166] M. Ghanei-Motlagh, M.A. Taher, Magnetic silver(I) ion-imprinted polymeric nanoparticles on a carbon paste electrode for voltammetric determination of silver(I), Microchim. Acta 184 (2017) 1691, doi:10.1007/s00604-017-2157-8.
[167] H. Yang, X. Liu, R. Fei, Y. Hu, Sensitive and selective detection of Ag^+ in aqueous solutions using Fe_3O_4@Au nanoparticles as smart electrochemical nanosensors, Talanta 116 (2013) 548, doi:10.1016/j.talanta.2013.07.041.
[168] M. Ebrahimi, J.B. Raoof, R. Ojani, Sensitive electrochemical DNA-based biosensors for the determination of Ag^+ and Hg^{2+} ions and their application in analysis of amalgam filling, J. Iran. Chem. Soc. 15 (2018) 1871, doi:10.1007/s13738-018-1384-1.
[169] G. Yan, Y. Wang, X. He, K. Wang, J. Su, Z. Chen, Z. Qing, A highly sensitive electrochemical assay for silver ion detection based on un-labeled C-rich ssDNA probe and controlled assembly of MWCNTs, Talanta 94 (2012) 178, doi:10.1016/j.talanta.2012.03.014.
[170] X. Liu, W. Li, Q. Shen, Z. Nie, M. Guo, Y. Han, W. Liu, S. Yao, The Ag^+-G interaction inhibits the electrocatalytic oxidation of guanine-a novel mechanism for Ag^+ detection, Talanta 85 (2011) 1603, doi:10.1016/j.talanta.2011.06.061.
[171] C. Chen, Q. Xie, L. Wang, C. Qin, F. Xie, S. Yao, J. Chen, Experimental platform to study heavy metal ion-enzyme interactions and amperometric inhibitive assay of Ag^+ based on solution state and immobilized glucose oxidase, Anal. Chem. 83 (2011) 2660, doi:10.1021/ac1031435.
[172] I.M. Rust, J.M. Goran, K.J. Stevenson, Amperometric detection of aqueous silver ions by inhibition of glucose oxidase immobilized on nitrogen-doped carbon nanotube electrodes, Anal. Chem. 87 (2015) 7250, doi:10.1021/acs.analchem.5b01224.
[173] K. Xu, G.A. Crespo, M. Cuartero, Subnanomolar detection of ions using thin voltammetric membranes with reduced exchange capacity, Sens. Actuat. B Chem. 321 (2020) 128453, doi:10.1016/j.snb.2020.128453.
[174] D. Yuan, M. Cuartero, G.A. Crespo, E. Bakker, Voltammetric thin-layer ionophore-based films: part 1. Experimental evidence and numerical simulations, Anal. Chem. 89 (2017) 586, doi:10.1021/acs.analchem.6b03354.
[175] M. Cuartero, G.A. Crespo, E. Bakker, Polyurethane ionophore-based thin layer membranes for voltammetric ion activity sensing, Anal. Chem. 88 (2016) 5649, doi:10.1021/acs.analchem.6b01085.
[176] G.A. Crespo, M. Cuartero, E. Bakker, Thin layer ionophore-based membrane for multianalyte ion activity detection, Anal. Chem. 87 (2015) 7729, doi:10.1021/acs.analchem.5b01459.
[177] N. Kolpakova, Z. Sabitova, V. Sachkov, R. Medvedev, R. Nefedov, V. Orlov, Determination of Au(III) and Ag(I) in carbonaceous shales and pyrites by stripping voltammetry, Minerals 9 (2019) 78, doi:10.3390/min9020078.
[178] D. Hernández, G. Ceprià, F. Laborda, J.R. Castillo, Detection and determination of released ions in the presence of nanoparticles: selectivity or strategy? Electroanalysis 31 (2019) 405, doi:10.1002/elan.201800597.
[179] J.C. Vidal, D. Torrero, S. Menes, A. de La Fuente, J.R. Castillo, Voltammetric sensing of silver nanoparticles on electrodes modified with selective ligands by using covalent and electropolymerization procedures. Discrimination between silver(I) and metallic silver, Microchim. Acta 187 (2020) 183, doi:10.1007/s00604-020-4139-5.
[180] W. Cheng, E.J. Stuart, K. Tschulik, J.T. Cullen, R.G. Compton, A disposable sticky electrode for the detection of commercial silver NPs in seawater, Nanotechnology 24 (2013) 505501, doi:10.1088/0957-4484/24/50/505501.
[181] E.J.E. Stuart, K. Tschulik, J. Ellison, R.G. Compton, Improving the rate of silver nanoparticle adhesion to 'sticky electrodes': stick and strip experiments at

a DMSA-modified gold electrode, Electroanalysis 26 (2014) 285, doi:10.1002/elan.201300452.
[182] K. Tschulik, R.G. Palgrave, C. Batchelor-McAuley, R.G. Compton, Sticky electrodes' for the detection of silver nanoparticles, Nanotechnology 24 (2013) 295502, doi:10.1088/0957-4484/24/29/295502.
[183] S. Steinberg, V. Hodge, B. Schumacher, W. Sovocool, Sampling for silver nanoparticles in aqueous media using a rotating disk electrode: evidence for selective sampling of silver nanoparticles in the presence of ionic silver, Environ. Monit. Assess. 189 (2017) 99, doi:10.1007/s10661-017-5809-6.
[184] G. Cepriá, W.R. Córdova, J. Jiménez-Lamana, F. Laborda, J.R. Castillo, Silver nanoparticle detection and characterization in silver colloidal products using screen printed electrodes, Anal. Methods 6 (2014) 3072, doi:10.1039/c4ay00080c.
[185] G. Cepriá, J. Pardo, A. Lopez, E. Peña, J.R. Castillo, Selectivity of silver nanoparticle sensors: discrimination between silver nanoparticles and Ag+, Sens. Actuat. B Chem 230 (2016) 25, doi:10.1016/j.snb.2016.02.049.
[186] C. Pérez-Ràfols, J. Bastos-Arrieta, N. Serrano, J. Manuel Díaz-Cruz, C. Ariño, J. de Pablo, M. Esteban, Ag nanoparticles drop-casting modification of screen-printed electrodes for the simultaneous voltammetric determination of Cu(II) and Pb(II), Sensors 17 (2017), doi:10.3390/s17061458.
[187] J. Bastos-Arrieta, A. Florido, C. Pérez-Ràfols, N. Serrano, N. Fiol, J. Poch, I. Villaescusa, Green synthesis of Ag nanoparticles using grape stalk waste extract for the modification of screen-printed electrodes, Nanomaterials 8 (2018) 946, doi:10.3390/nano8110946.
[188] P.M. Carvalho, M.R. Felicio, N.C. Santos, S. Goncalves, M.M. Domingues, Application of light scattering techniques to nanoparticle characterization and development, Front. Chem. 6 (2018) 237, doi:10.3389/fchem.2018.00237.
[189] S. Bykkam, M. Ahmadipour, S. Narisngam, V.R. Kalagadda, S.C. Chidurala, Extensive studies on X-ray diffraction of green synthesized silver nanoparticles, Adv. Nanopart. 04 (2015) 1, doi:10.4236/anp.2015.41001.
[190] P. Zhang, I. Wyman, J. Hu, S. Lin, Z. Zhong, Y. Tu, Z. Huang, Y. Wei, Silver nanowires: synthesis technologies, growth mechanism and multifunctional applications, Mater. Sci. Eng. B 223 (2017) 1, doi:10.1016/j.mseb.2017.05.002.
[191] E. Bahcelioglu, H.E. Unalan, T.H. Erguder, Silver-based nanomaterials: a critical review on factors affecting water disinfection performance and silver release, Crit. Rev. Environ. Sci. Technol. 223 (2020) 1, doi:10.1080/10643389.2020.1784666.
[192] C.A. Li, D. Kim, Electrochemical monitoring of colloidal silver nanowires in aqueous samples, Analyst 140 (2015) 6705, doi:10.1039/c5an01264c.
[193] Z. Koudelkova, T. Syrovy, P. Ambrozova, Z. Moravec, L. Kubac, D. Hynek, L. Richtera, V. Adam, Determination of zinc, cadmium, lead, copper and silver using a carbon paste electrode and a screen printed electrode modified with chromium(iii) oxide, Sensors 17 (2017) 1832, doi:10.3390/s17081832.
[194] R. Zhiani, M. Ghanei-Motlag, I. Razavipanah, Selective voltammetric sensor for nanomolar detection of silver ions using carbon paste electrode modified with novel nanosized Ag(I)-imprinted polymer, J. Mol. Liq. 219 (2016) 554, doi:10.1016/j.molliq.2016.03.052.
[195] Q. Liu, F. Wang, Y. Qiao, S. Zhang, B. Ye, Polyaniline Langmuir–Blodgett film modified glassy carbon electrode as a voltammetric sensor for determination of Ag^{+} ions, Electrochim. Acta. 55 (2010) 1795, doi:10.1016/j.electacta.2009.10.069.